https://ntrs.nasa.gov/search.jsp?R=19720006177 2020-03-23T14:58:14+00:00Z

FACILITY FORM 602
N72-13826 (ACCESSION NUMBER)
(THRU)
(PAGES)
(CODE)
(NASA CR OR TMX OR AD NUMBER)
(CATEGORY)

SPACE SCIENCES LABORATORY

ATS-10743

Final Scientific Report

LEAR TRACKS IN LUNAR SAMPLES

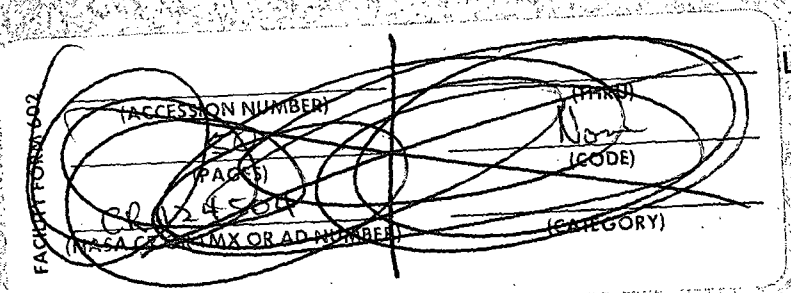

NASA Contract NAS 9-10488

Covering the Interval

December 1, 1969, to January 1, 1971

Principal Investigator: Prof. P. B. Price

November 1971

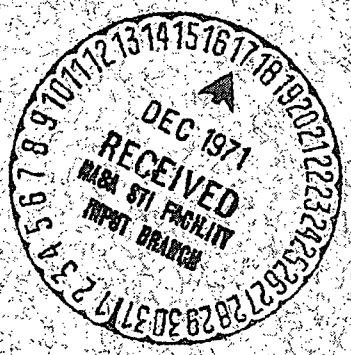

Space Sciences Laboratory Series 12 Issue 84

UNIVERSITY OF CALIFORNIA, BERKELEY

CASE FILE COPY

Space Sciences Laboratory
University of California
Berkeley, California 94720

Final Scientific Report

NUCLEAR TRACKS IN LUNAR SAMPLES

NASA Contract NAS 9-10488

November 1971

Principal Investigator: Professor P. B. Price

Space Sciences Laboratory Series 12 Issue 84

NUCLEAR TRACKS IN LUNAR SAMPLES

Progress Report for Interval

September 15, 1970 to September 15, 1971

I. Publications during the interval (copies attached in Appendix A).

1. D. J. Barber, I. D. Hutcheon and P. B. Price, "Extralunar Dust in Apollo Cores?", Science 171, 372 (1971).

2. P. B. Price, I. D. Hutcheon, R. Cowsik and D. J. Barber, "Enhanced Emission of Iron Nuclei in Solar Flares," Phys. Rev. Letters 26, 916 (1971).

3. P. B. Price, R. S. Rajan and E. K. Shirk, "Ultra-heavy Cosmic Rays in the Moon," Proc. 2nd Lunar Science Conference, Vol. 3, in press.

4. D. J. Barber, R. Cowsik, I. D. Hutcheon, P. B. Price and R. S. Rajan, "Solar Flares, the Lunar Surface and Gas-Rich Meteorites," Proc. 2nd Lunar Science Conference, Vol. 3, in press.

5. H.-R. Wenk and G. L. Nord, "Lunar Bytownite from Sample 12032,44," Proc. 2nd Lunar Science Conference, Vol. 1, in press.

6. H.-R. Wenk and K. N. Raymond, "Structure Refinements of Four Olivines," Amer. Min., in press.

7. D. J. Barber, "Mounting Methods for Mineral Grains to be Examined by High Resolution Electron Microscopy," Amer. Min., in press.

8. D. J. Barber and P. B. Price, "Solar Particle Tracks in Lunar and Meteoritic Minerals," Proc. 25th Anniversary Meeting of EMAG, Inst. Physics, 1971.

II. Review papers written during the interval (not attached)

1. P. B. Price and R. L. Fleischer, "Identification of Energetic Heavy Nuclei with Solid Dielectric Track Detectors: Applications to Astrophysical and Planetary Studies," Ann. Rev. Nucl. Sci. 21, 1971.

2. R. Cowsik and P. B. Price, "Origins of Cosmic Rays," Physics Today, October, 1971.

III. New, unpublished results

1. Search for spontaneously fissioning superheavy elements

During a one-month period in February, 1971, 2.8 kg of Apollo 11 and 12 fines in special, sealed cans were studied by low-level neutron

detectors under 1000 ft of rock in the Bay Area Rapid Transit tunnel near Berkeley. The electronics equipment was operated by S. G. Thompson, E. Cheifetz, R. C. Jared and E. R. Giusti of Lawrence Radiation Laboratory and was capable of detecting spontaneous fission events in which several neutrons were simultaneously emitted: In fission of uranium the mean neutron multiplicity is about 3; in fission of hypothetical element 114 the expected multiplicity is 10 to 12. No events with a high neutron-multiplicity were detected and no evidence for super-heavy elements brought into the lunar dust in the cosmic radiation was found. It was exceedingly time-consuming to set up the experiment and arrange for acceptable containers to be built and for 2.8 kg of fines to be carried between MSC and Berkeley. We have no plans to publish these negative results.

2. Identification of heavy ion tracks in minerals and glasses

Using 10 MeV/nucleon Kr beams from the Berkeley Heavy Ion Accelerator and 6 MeV/nucleon Zn beams from the Dubna cyclotron in the Soviet Union, we are making progress in relating the appearance of an etched track to the atomic number and velocity of the ion that left the track. We have found that the etching rate along a track in a mineral and in a glass is a monotonic function of ionization rate and thus that particle identification should be possible by the same method we developed for plastic detectors.

Our annealing studies show that the etching rate of Fe tracks is reduced after only a few hours of annealing at temperatures as low as 300° C. With the completion of these studies we can predict the effects of a prolonged exposure at the lunar surface temperature.

These experiments have several important consequences--for assessing the claims by Bhandari et al.--that fission tracks of superheavy elements have been found in lunar fines; for identifying cosmic rays with $Z > 26$; for testing our recent idea for studying cosmic ray flux variations in the last 10^8 years;

and for identifying solar flare particles in the Surveyor glass. Some of these results will appear in the review paper by Price and Fleischer cited above.

3. The lunar regolith

Using a 650 kev electron microscope, we previously found extremely high densities ($>10^{11}/cm^2$) of solar flare tracks in micron-size grains at all depths in core samples from Apollo 11 and 12. We also found that more than 90% of large grains (diameter >50 microns) at several depths had track densities greater than $10^8/cm^2$. Among the possible explanations, we suggested that a certain fraction of all depths could have acquired their high track densities as micrometeorites orbiting the sun, before finally reaching the moon.

APPENDIX A

Publications on Lunar Sample Studies

Reprinted from
29 January 1971, Volume 171, pp. 372-374

SCIENCE

Extralunar Dust in Apollo Cores?

D. J. Barber, I. Hutcheon and P. B. Price

Copyright© 1971 by the American Association for the Advancement of Science

Extralunar Dust in Apollo Cores?

Abstract. *Densities of nuclear tracks exceed 10^{11} per square centimeter in several percent of the micrometer-size silicate grains from all depths in the 12- and 60-centimeter lunar cores. Either these grains were irradiated in space as extralunar dust or the ratio of iron to hydrogen in low-energy (about 1 million electron volts per nucleon) solar particles is orders of magnitude higher than in the photosphere.*

With the Berkeley 650-kv electron microscope we have found track densities up to and exceeding 3×10^{11} per square centimeter in small silicate crystals (diameter ~0.5 to ~3 μm) from all depths in Apollo 11 and 12 cores. We will discuss the constraints that these remarkable observations place on the origin of the lunar dust.

By diffraction contrast, tracks are visible in silicate grains (Fig. 1) but must be observed through an amorphous layer (~1000 Å thick) that is suggestive of solar wind radiation damage. We find that a very light etch removes this layer and improves track visibility. A carbon film is evaporated onto a microscope slide containing grains of less than ~3 μm, is stripped off the slide, and is then floated on a solution of $2HF : 1H_2SO_4 : 280H_2O$ for 30 seconds. In addition to serving as a support for the tiny grains, the film replicates their original shapes, so that the decrease in grain diameters resulting from etching can be followed. This very weak etch solution satisfactorily reveals tracks in all the common lunar silicates —pyroxenes, feldspars, and olivines— without destroying glassy grains or other minerals.

In Fig. 2 etched tracks in pyroxene and olivine as identified by electron diffraction are shown. The slitlike shapes of the etched tracks in Fig. 2B are characteristic of olivine (*1*). The shapes of the etched lines, their angular and length distributions, the occasional gradients across a grain diameter, their annealing behavior (no tracks being visible either with or without etching after heating to ~500°C), and the absence of such lines in nontrack-recording crystals (ilmenite, for example) identify them as nuclear tracks (*2*). Other kinds of defects in lunar grains will not be discussed here.

From our observations of well over 1000 etched grains, we estimate that, *at all depths*, at least 15 percent of silicate grains with diameters of 0.5 to 3 μm have track densities exceeding 10^{10} per square centimeter. About two-thirds of the grains are glass (which must be etched under different conditions) and nontrack-recording minerals, and they are excluded from this analysis. At least 3 percent of the 0.5- to 3-μm silicate grains *at all depths* have $>10^{11}$ track/cm^2. The percentage is probably even higher, but track densities greater than $\sim 4 \times 10^{11}$ per square centimeter are simply not resolvable.

X-ray powder patterns of unetched 0.5- to 3-μm grains, taken by H. R. Wenk, provide evidence of severe strains and support our contention that the grains have been severely damaged by radiation (*3*).

Previous workers, who studied much larger grains (diameter $\gtrsim$ 100 μm) with optical microscopy (*4–6*), scanning electron microscopy (*4*), and a replication technique (*5*), found a wide distribution of track densities ranging from $< 10^6$ per square centimeter up to their limit of resolution, $\sim 3 \times 10^9$ per square centimeter, at all depths in the 10.5- and 12.5-cm Apollo 11 cores (*4–6*). With optical microscopy, we find that the fraction of large ($\gtrsim$ 50 μm) silicate grains containing $> 10^8$ track/cm^2 slowly decreases from ~95 percent at the surface to ~75 percent at a depth of 60 cm.

We believe, with previous workers (*4–7*), that many of the grains with track densities up to a few times 10^9 per square centimeter could have been chipped off surface rocks by meteorite

Fig. 1. Unetched crystal of clinopyroxene containing 7×10^{10} track/cm^2 which are attributed to nuclei with atomic number $Z \approx 26$ emitted in solar flares. This crystal, like those in Fig. 2, was selected from the residue remaining on a glass slide after part of an Apollo 12 core sample was poured onto the slide and then poured off (× 73,500).

impact and could have accumulated their tracks while residing on the surface before being stirred into the soil by later impacts.

Our main purpose in this report, however, is to point out the difficulty of accounting for small grains with track densities of $\geqslant 10^{10}$ per square centimeter throughout a depth of 60 cm. The maximum track density expected from either spontaneous or induced fission of uranium or of an extinct element, or from galactic cosmic rays or their spallation recoils, falls orders of magnitude short of that observed. The most reasonable origin of the tracks is irradiation by heavy nuclei emitted by the sun with energies of ~ 1 Mev per nucleon. This is about 10^3 times the average energy of solar wind ions and is probably associated with solar flares. Studies of solar flare tracks (*4*, *7*, *8*) and of flare-induced radioactivity (*9*) in lunar rocks with measured surface residence times of $\sim 10^7$ years strongly suggest that the average level of solar activity has not changed drastically over the last 10^7 years. By using either an average energy spectrum $\propto E^{-3}$ [suggested by recent satellite measurements (*10*)] or an average rigidity spectrum $\propto e^{-R/100\ \mathrm{Mv}}$, we reach the same conclusion that a grain within ~ 10 μm of the surface will accumulate 10^{11} track/cm^2 in about 10^7 years. At a depth of 100 μm the required irradiation time is greater than 10^8 years. Because of the steepness of the solar particle energy spectrum, the most rapid accumulation occurs by exposing each grain in the top 10 μm of soil at least once. To irradiate 10 percent of the grains in the top 60 cm of soil with 10^{11} track/cm^2 would require more than 6×10^{10} years at the present level of solar activity, if the Fe/H ratio in solar particles and in the photosphere is assumed to be the same, $\sim 4 \times 10^{-5}$. Since there is no indication of a decrease of track density with depth, a much greater thickness than 60 cm presumably contains high track densities; and an even longer irradiation time would be required to produce them.

In order for the grains to have acquired their high track densities while on or near the lunar surface in a time less than the age of the solar system, either we must postulate that the irradiation occurred at an early stage in the evolution of the sun, when its power output in solar flares was orders of magnitude higher than it has been for the last $\sim 10^7$ years, or we must postulate that the Fe/H ratio in low-energy solar particles is several orders of magnitude higher than in the photosphere.

The difficulty disappears if the tracks accumulated in grains that orbited the sun but gradually spiraled in, owing to the Poynting-Robertson effect, until they were swept up by the moon and built up a lunar soil. Although grains that collide with rocks would be destroyed (giving rise to glass-lined craters), those that impinge with minimum velocity (~ 2 km/sec) on a fluffy, porous soil of like grains can transfer much of their energy to those grains, and portions of them should survive. Stored tracks are known to be unaffected by shock pressures up to at least 150 kb, which corresponds to impact velocities considerably higher than 2 km/sec.

Grains of initial radius 100 μm and initial perihelion 2.8 A.U. (corresponding to the asteroidal belt) would have a Poynting-Robertson lifetime of 2×10^6 years if they were perfectly absorbing or reflecting and would have a considerably longer lifetime if they were transparent. In 10^6 to 10^7 years they would accumulate 10^{10} to 10^{11} track/cm^2 in their outer 20 μm or so. Since the Poynting-Robertson lifetime is proportional to radius, very small grains could not accumulate high track densities, and we would attribute the highest track densities to fragments from the outer portions of grains of radius $\gtrsim 100$ μm that fractured on impact.

Our observations do not allow us to distinguish whether high track density grains have been added to the soil on a continuing basis or only during the early history of the moon. If addition has continued, we would expect the mineralogy and chemistry of those grains and of meteorites to be similar. From a gross analysis of enriched concentrations of certain trace elements, Keays *et al.* (*11*) conclude that ~ 1 percent of the lunar soil is of meteoritic origin. It would be interesting to see whether the meteoritic fraction is larger for small grains of diameter < 3 μm. It would also be interesting to search Pacific Ocean sediments for grains with high track densities, because their existence would provide evidence of a continuing infall.

The concentration of rare gases of solar origin in the lunar soil is an inverse function of grain size (*12–14*). The flux of solar wind gases, which penetrate less than ~ 1000 Å below the surface, is so high that the gas concentration near the surfaces of grains quickly reaches a saturation level in a time less than $\sim 10^3$ years (*13*) and

Fig. 2. Etched crystals. (A) Clinopyroxene containing 3×10^{11} track/cm^2 from Apollo 12 core; etched for 30 seconds in 2HF : $1H_2SO_4$: $280H_2O$ ($\times$ 136,500). (B) Olivine containing 1.2×10^9 track/cm^2 from Apollo 12 core; etched for 1 minute in 2HF : $1H_2SO_4$: $45H_2O$ ($\times$ 23,800).

thus does not provide a test of the hypothesis of extralunar origin. A selective study of the more deeply seated gases produced in solar flares might, however, provide such a test. By leaching away the surfaces of specific silicate grains, one might be able to study the solar flare gas content of the interior portions. However, because of possible diffusion effects, a rare gas study would be more difficult to interpret than our track evidence.

Spallogenic nuclides are produced by cosmic-ray bombardment down to a depth of ~ 1 m. From analysis of stable spallogenic rare gases, various groups have inferred an exposure age of $\sim 5 \times 10^8$ years for the soil (*13–15*). This is not its absolute age but refers to the time spent within ~ 1 m of the surface. Provided deep stirring has occurred, this age can be compatible either with an early origin of the soil or with continuing production.

An extralunar origin of the grains with high track densities is consistent with Gold's dust model (*16*) of the origin of the lunar surface. We believe that the attractive features of his model outweigh the difficulties. An important and testable consequence of the model is that the grains with high track densities should also occur at much greater depths than 60 cm, perhaps orders of magnitude deeper. The desirability of a 4-m core sample such as had been planned on Apollo 13 is obvious.

The most popular model of the origin of the soil is that a regolith accumulates on a solid bedrock by comminution of chips of the bedrock resulting from meteorite impacts (*17*). Our explanation for the high track densities could be compatible with this impact model only if the extralunar infall had continued over several billion years, so as to maintain a large fraction of infallen grains with very high track densities. We believe that the simplest explanation of our results is that much of the soil developed from infall of extralunar particles (*18*).

Note added in proof: We have now directly measured the energy spectrum of Fe nuclei over a 2.5-year period by analyzing tracks recorded in a glass filter in the Surveyor 3 camera that was brought back from the moon by the Apollo 12 astronauts. We have found that the Fe/H ratio in low-energy solar particles is much higher than we had assumed from the photospheric ratio. The high Fe flux reduces but does not entirely eliminate the difficulty of accounting for the grains with high track density. An extralunar origin of part of the soil is still consistent with our observations.

D. J. BARBER*
I. HUTCHEON
P. B. PRICE
Department of Physics, University of California, Berkeley 94720

References and Notes

1. M. Maurette, P. Pellas, R. M. Walker, *Nature* **204**, 821 (1964).
2. Etched nuclear tracks of natural origin were first seen by P. B. Price and R. M. Walker [*Nature* **196**, 732 (1962)], who observed spontaneous fission tracks in terrestrial micas by electron microscopy. Etched tracks of heavy cosmic rays in extraterrestrial bodies (meteorites) were first observed by optical microscopy and reported by Maurette *et al.* [see (*1*)].
3. Further details of the x-ray analysis will be reported elsewhere.
4. G. Crozaz, U. Haack, M. Hair, M. Maurette, R. Walker, D. Woolum, in *Proceedings of the Apollo 11 Lunar Science Conference* (Pergamon, New York, 1970), vol. 3, p. 2051.
5. R. L. Fleischer, E. L. Haines, H. R. Hart, R. T. Woods, G. M. Comstock, *ibid.*, p. 2103.
6. D. Lal, D. Macdougall, L. Wilkening, G. Arrhenius, *ibid.*, p. 2295.
7. P. B. Price and D. O'Sullivan, *ibid.*, p. 2351.
8. D. J. Barber and P. B. Price, in preparation.
9. J. R. Arnold, private communication.
10. J. Hsieh and J. A. Simpson, private communication.
11. R. R. Keays, R. Ganapathy, J. C. Laul, E. Anders, G. F. Herzog, P. M. Jeffery, *Science* **167**, 490 (1970).
12. D. Heymann, A. Yaniv, J. A. S. Adams, G. E. Fryer, *ibid.*, p. 555.
13. P. Eberhart *et al.*, *ibid.*, p. 558.
14. T. Kirsten, F. Steinbrunn, J. Zähringer, *ibid.*, p. 571.
15. K. Marti, G. W. Lugmair, H. C. Urey, *ibid.*, p. 548; R. O. Pepin, L. E. Nyquist, D. Phinney, D. C. Black, *ibid.*, p. 550; C. M. Hohenberg, P. K. Davis, W. A. Kaiser, R. S. Lewis, J. H. Reynolds, in *Proceedings of the Apollo 11 Lunar Science Conference* (Pergamon, New York, 1970), vol. 2, p. 1283.
16. T. Gold, "The Nature of the Surface of the Moon" (preprint 380, Cornell University Center for Radiophysics and Space Research, Ithaca, N.Y., 1970); ———, *Proc. Amer. Phil. Soc.*, in press; ——— and S. Soter, *Science* **169**, 1071 (1970).
17. E. M. Shoemaker *et al.*, in *Proceedings of the Apollo 11 Lunar Science Conference* (Pergamon, New York, 1970), vol. 3, p. 2399.
18. After the manuscript of this report was completed, we learned of high voltage electron microscope observations of lunar crystals with track densities up to 10^{11} per square centimeter [J. Borg, J. C. Dran, L. Durrieu, C. Jouret, and M. Maurette, *Earth Planet. Sci. Lett.* **8**, 379 (1970)]. They used an acid solution that was approximately 70 times as strong as the one we used, but they reported that the tracks in their grains were not etched. It is possible that all silicates were completely dissolved in their solution, leaving only mineral grains that would require a different chemical etchant. One of their photographs was of a cristobalite grain, which we believe would not be etched in their solution.
19. We are greatly indebted to F. Borden for experimental assistance. Supported by NASA contract NAS 9-10488 and by AEC contract AT(04-3)-34.
* On leave from Department of Physics, Essex University, Colchester, U.K.

8 October 1970

Enhanced Emission of Iron Nuclei in Solar Flares

P. B. Price, I. Hutcheon, R. Cowsik,* and D. J. Barber†
Department of Physics, University of California, Berkeley, California 94720
(Received 18 January 1971)

Etched tracks in an Apollo-12 spacecraft window and a Surveyor-3 camera-lens filter give the interplanetary Fe energy spectra from ~1 to ~30 MeV/nucleon during 1967-1969. The strongly energy-dependent Fe/He ratio suggests that heavy nuclei are preferentially emitted from accelerating regions because of their low ionization state and high magnetic rigidity. The Fe fluxes give rise to extremely high track densities that we have observed in lunar soil.

From an analysis of tracks in a window of the Apollo-12 spacecraft and in a glass filter from the Surveyor-3 camera brought back from the moon, we have determined the spectrum of Fe nuclei from ~1 to ~30 MeV/nucleon in interplanetary space during the interval 24 April 1967 to 24 November 1969 and in the last 10 days of this interval. The intensity and spectral slope were higher than we expected on the basis of studies of α particles by other investigators[1,2] during that period and the assumption of an Fe/He ratio equal to that in the solar photosphere.[3-5] In addition to their relevance for solar physics, our results may have important consequences for galactic cosmic-ray processes. They also contribute importantly to the extremely high track densities we have observed in the lunar soil[6] and allow us to estimate the rate of erosion of lunar rocks.

The silica glass windows on the Apollo-12 command module were exposed to space with an effective recording solid angle of ~1 sr from 14 to 24 November 1969. A neutral-density flint glass filter over the lens system on the Surveyor-3 camera had an ~0.7-sr effective view of space during a 2.5-yr period while it resided on the lunar surface.

We received one Apollo-12 window and a small piece of the Surveyor camera filter for study. In both types of glass, tracks of heavily ionizing particles can be revealed by chemical etching.[7,8] The visibility of etched tracks depends on ionization rate and increases rapidly with atomic number. From bombardments of glasses with heavy ions we conclude that ions with $Z \lesssim 16$ record with very low efficiency and leave tracks which etch into pits with a very low visibility when viewed in an optical microscope. For this reason, and since the solar abundance of ions with >16 is strongly peaked at Fe, glass detectors discriminate strongly in favor of Fe. Ions of Fe with energy below ~6 MeV/nucleon, i.e., a range less than ~40 μm, have a sufficiently high ionization rate that they will leave tracks that can be etched into easily recognizable conical pits. Ions of Fe of higher energy have too low an ionization rate to leave etchable tracks at the surface, but the lower energy portions of their trajectories can be exposed by grinding or chemically etching away some of the glass, and these portions can then be detected by additional etching. The depth in the glass at which an Fe track is recorded is thus a measure of its energy.

By means of a sequence of etching (with dilute HF) and grinding operations, densities of etch pits were measured throughout the entire 3-mm Surveyor glass thickness, corresponding to Fe energies from ~1 to ~100 MeV/nucleon, and at the top surface of the Apollo-12 window. Figure 1 summarizes the measurements. In the same figure is shown the etch-pit distribution we would expect if Fe and He were emitted from the sun in the ratio of their photospheric abundances. That distribution was calculated using the α-particle energy spectrum measured during the same 2.5-yr period by solid state detectors on IMP 4 and 5 by Lanzerotti[1] and by Hsieh and Simpson.[2] Seven major solar flares contributed most of the flux. The α-particle spectrum scaled down by the recently redetermined[3-5] solar ratio $(\mathrm{Fe/He})_\odot \approx 2\times10^{-4}$ was used as the input for the calculation.

The large difference between the observed and predicted track densities was completely unexpected. After converting the observed track density distribution to a rigidity (or energy) distribution, we obtain the important result that at low rigidity (or energy) the solar-particle Fe/He ratio is much higher than the photospheric abundance ratio but decreases with increasing rigidity until it approaches the photospheric value at a rigidity of ~500 MV (~25 MeV/nucleon for Fe). In the only previous observations of solar particles with $Z > 20$, Bertsch, Fichtel, and Keames[9] found 23 tracks of Fe-group nuclei in nuclear emulsions exposed in a 5-min rocket flight dur-

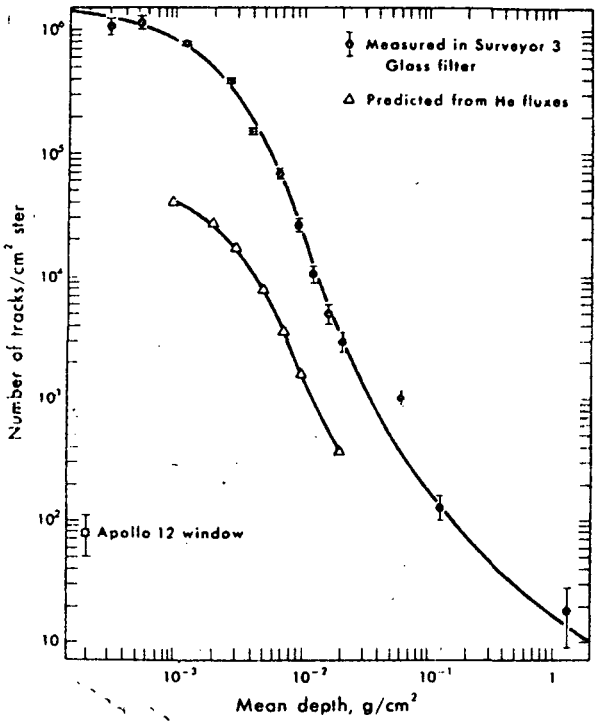

FIG. 1. Observed densities of Fe tracks penetrating to a given depth of Surveyor-3 glass and Apollo-12 glass compared with densities predicted assuming Fe/He solar particle ratio is the same as the photospheric ratio. The tracks are made visible by chemical etching if their residual range at a glass surface is less than ~40 μm.

ing the flare of 2 September 1966. They found Fe/He $\approx 2\times10^{-4}$ at $E > 24.5$ MeV/nucleon, which is not inconsistent with our results. However, one should keep in mind the possibility that over a 2.5-yr period there may be a significant contribution by galactic cosmic rays with a much higher Fe/He ratio at energies beyond ~25 MeV/nucleon.

During the period 14 to 24 November 1969, in which the Apollo-12 windows were exposed, a small interplanetary enhancement occurred, contributing a flux of α particles only $\sim10^{-4}$ times the total contribution over the previous 2.5-yr period (Lanzerotti[10]). The track counts corresponding to very low-energy Fe nuclei in the Apollo-12 window indicate that the low-energy Fe flux during those 10 days was $\sim7\times10^{-5}$ times the total over 2.5 yrs, in good agreement with the relative α-particle contribution. This result supports the assertion that the low-energy Fe tracks are of solar origin and are not simply an accumulated background of low-energy galactic Fe nuclei.

Our results represent the first evidence that heavy nuclei can be preferentially emitted from a source of energetic particles. Previously Fichtel and co-workers[11,12] had found such a striking similarity between the abundances of energetic solar particles and of the photosphere that the earlier suggestion by Korchak and Syrovatskii[13] that heavy nuclei may be preferentially accelerated has largely been forgotten. Admittedly their mechanism, which applies when the acceleration rate is small, does not account for the strong enhancement of Fe observed by us because acceleration of particles in solar flares takes place so rapidly that the energy loss suffered through ionization by the ions during the acceleration phase is negligible. Instead, we attribute the enhancement to preferential leakage of incompletely ionized heavy nuclei from the accelerating region.

The effective charge of an ion depends on its velocity as $Z^* = Z[1-\exp(-125\beta/Z^{2/3})]$. From this it can be seen that H and He are completely stripped of their electrons even at an energy of ~1 MeV/nucleon, whereas Fe ions have an effective charge of only ~13 at 1 MeV/nucleon, increasing to ~24 at 15 MeV/nucleon and becoming very nearly equal to the nuclear charge, 26, only at energies above ~40 MeV/nucleon. Thus, heavy ions have rigidities higher by a factor $\sim Z^*/Z$ than that of an α particle at the same energy per nucleon.

Now, if the probability of escape of the accelerated particles is a strong function of their rigidity, one can understand the enhanced Fe fluxes. It appears reasonable that heavy ions, which have a higher rigidity because of their smaller effective charge, should leak out preferentially from the flare regions relative to α particles and protons of the same energy per nucleon. This preferential escape, which is a consequence of retention of some electrons around a heavy nucleus, should vanish at those high energies at which all the nuclei of interest are completely ionized. All previous observations[9,11,12] of solar-particle composition have been made at sufficiently high energies that no enhancement would be expected. It is interesting to speculate on the possibility, as previously suggested by Davis,[14] that this process of enhancement of heavy nuclei may operate as the injection mechanism for the galactic cosmic rays which are later accelerated to high energies. Thus the overabundance of heavy nuclei in the cosmic rays may not be entirely indicative of source composition but may be partly a consequence of preferential leakage

from the source.

It should also be interesting to solar-particle physicists to mention that the solar α-particle and proton intensities summed over the 2.5-yr period, when plotted as differential rigidity spectra, have the form $\sim A_i \exp(-R/R_0)$, with the same value of R_0 for protons and α particles. Their relative intensities, A_i, scale by a factor ~2, consistent with model calculations of their photospheric abundance ratio. This agreement is consistent with our model of the enhanced Fe emission because both H and He should be completely stripped at energies above ~1 MeV/nucleon.

Turning now to some quite different implications of our results, we can use the track-density measurements in Fig. 1 to draw interesting conclusions about events in the distant past, assumming that the average level of solar activity has remained roughly constant over geologic time:

(1) Rocks exposed undisturbed on the lunar surface for 10^7 years would accumulate about 6×10^{12} tracks/cm in the top 10 μm of their thickness. Accelerator bombardments of certain minerals with neon and argon ions[15] show that extensive strains and fractures occur at track densities $\sim10^{12}/\mathrm{cm}^2$. Summing the contributions of all solar particles with $Z \gtrsim 10$, we conclude that the rate of radiation-induced erosion by fracturing of surface grains is likely to be $\sim10^{-9}$ cm/yr. In current unpublished electron microscope studies of Fe track densities as a function of depth in rocks exposed on the lunar surface for $\sim10^7$ yr, we find a maximum track density of $\sim10^{10}/\mathrm{cm}^2$ at the very surface. The difference between the observed gradient of track density and the gradient to be expected from Fig. 1 is attributed to various erosion processes including atomic sputtering by solar wind ions, cratering by micrometeorite bombardment, and flaking of radiation-damaged grains. We conclude that the total erosion rate of rocks that survive for $\sim10^7$ yr on the lunar surface is $\sim3\times10^{-8}$ cm/yr. This limit agrees very well with the present estimated erosion rate by micrometeorites, $(1\text{-}2)\times10^{-8}$ cm/yr,[15] and allows us further to conclude that the present micrometeorite flux measured now on satellite detectors is nearly the same as the long-term average value.

(2) The lunar soil should contain heavily irradiated small grains, some with track densities of $\sim10^{12}/\mathrm{cm}^2$ that have flaked off of radiation-damaged rock surfaces and some that were irradiated while residing at the top of the soil layer. Given a soil of depth ~5 m that has accumulated over $\sim3.5\times10^9$ yr and has been frequently stirred by meteoritic impacts, we expect an average track density of $\sim10^{10}/\mathrm{cm}^2$ in grains of diameter less than about 10^{-3} cm. Because of the steepness of the solar Fe energy spectrum, larger grains should show visible gradients. We have previously reported all of these features,[6] but were unable to account satisfactorily for the extremely high track densities without knowing the solar-flare Fe spectrum. The steep track density gradient in Fig. 1 now provides a reasonable, quantitative explanation for the bulk of the observations.

This work was supported by the U. S. Atomic Energy Commission, by the National Aeronautics and Space Administration, and by the National Science Foundation. We are indebted to Richard Baldwin of National Aeronautics and Space Administration for arranging for the loan of an Apollo-12 window, to Neil Nickle of Jet Propulsion Laboratory for supplying us with the Surveyor-3 glass filter, and to Lou Lanzerotti and K. C. Hsieh for supplying us with their unpublished data.

---

*On leave from Tata Institute of Fundamental Research, Bombay, India.

†On leave from Department of Physics, Essex University, Colchester, U. K.

[1]L. J. Lanzerotti, World Data Center A, Report No. UAG-5, February 1969 (unpublished), p. 56; L. J. Lanzerotti and C. M. Soltis, World Data Center A, Report No. UAG-8, March 1970 (unpublished), p. 198; L. J. Lanzerotti, World Data Center A, Report No. UAG-9, April 1970 (unpublished), p. 34.

[2]K. C. Hsieh and J. A. Simpson, Astrophys. J. 162, L191 (1970); also unpublished results (private communication).

[3]T. Gärz, M. Kock, J. Richter, B. Baschek, H. Holweger, and A. Unsöld, Nature 223, 1254 (1969).

[4]S. J. Wolnik, R. O. Berthel, and G. W. Wares, Astrophys. J. 162, 1037 (1970).

[5]J. E. Ross, Nature 225, 610 (1970).

[6]D. J. Barber, I. Hutcheon, and P. B. Price, to be published.

[7]R. L. Fleischer and P. B. Price, J. Appl. Phys. 34, 2903 (1963).

[8]R. L. Fleischer, P. B. Price, and R. T. Woods, Phys. Rev. 188, 563 (1969).

[9]D. L. Bertsch, C. E. Fichtel, and D. V. Reames, Astrophys. J. 157, L54 (1969).

[10]L. J. Lanzerotti, private communication.

[11]S. Biswas and C. E. Fichtel, Space Sci. Rev. 4, 709 (1965).

[12]N. Durgaprasad, C. E. Fichtel, D. E. Guss, and D. V. Reames, Astrophys. J. 154, 307 (1968).

[13]A. A. Korchak and S. I. Syrovatskii, Dokl. Akad. Nauk SSSR 122, 792 (1958) [Sov. Phys. Dokl. 3, 983 (1958)].
[14]L. Davis, Jr., in *Space Sciences*, edited by D. P. Le Galley (Wiley, New York, 1963), Chap. 12.
[15]M. Seitz, M. C. Wittels, M. Maurette, and R. M. Walker, to be published.
[16]F. Hörz, J. B. Hartung, and D. E. Gault, Lunar Science Institute Report No. 09 (unpublished), and in Proceedings of the Appollo 12 Lunar Science Conference, Houston, Texas, 11-14 January 1971 (to be published).

(3)

Proceedings of the Second Lunar Science Conference, Vol. 3, pp. [redacted]
The M.I.T. Press

Ultra-heavy cosmic rays in the moon

P. B. PRICE, R. S. RAJAN and E. K. SHIRK
Department of Physics, University of California, Berkeley, California 94720

(*Received* 22 *February* 1971; *accepted in revised form* 30 *March* 1971)

Abstract—Large (> 1 mm) pigeonite crystals in lunar rock 12021 contain tracks up to at least 1 mm long, some going through their entire thickness. We use these tracks to set upper limits of $\sim 3 \times 10^{-8}$/cm^2 year on the flux of multiply charged magnetic monopoles produced in high energy cosmic ray interactions in the moon and of $\sim 10^{-4}$/cm^2 year on the flux of super-heavy cosmic rays with $Z \geq 110$ stopping within moon crystals. We use the track length distributions to infer the existence of a finite flux of cosmic ray nuclei with $Z > 82$ over the last $\sim 10^7$ years. We conclude that the overall abundance pattern appears not to have changed drastically in 10^7 years. We use a 10 MeV/N Kr^{84} ion calibration to provide new information on the response of pigeonite crystals to monopoles and ultra-heavy nuclei. We briefly discuss reports by other workers of the existence of long-lived super-heavy elements.

INTRODUCTION

THE INITIAL motivation for this paper was to discuss the possibility that some of the extremely long tracks that we have discovered (BARBER *et al.*, 1971) in rock 12021 might have been made by magnetic monopoles or by super-heavy cosmic rays with $Z > 110$. Since the Apollo 12 conference we have been able to study the response of moon crystals to a beam of 10 MeV/N Kr^{81} ions. These results, which we describe below, show that the longest tracks need not have been produced by transuranic cosmic rays but could have been produced by nuclei with atomic number $Z \leq 92$.

In view of two very recent developments, we wish to emphasize that our Kr calibration does not rule out the possibility that our longest tracks were left by super-heavy cosmic rays, and we shall use them to obtain a limit on the flux of high energy nuclei with $Z > 92$ coming into the solar system. The developments to which we refer are the recently reported discovery (MARINOV *et al.*, 1971) of element 112, eka-mercury, with a half-life greater than a few months, which qualifies it for a position in the "island of stability," and the announcement at the Apollo 12 conference (BHANDARI *et al.*, 1971b) of evidence for the existence of spontaneous fission tracks from super-heavy elements that once existed in certain grains of the lunar soil.

The existence of cosmic rays with $Z > 30$ had previously been established from studies of fossil tracks in meteorites (FLEISCHER *et al.*, 1967) and confirmed by observations in large area emulsion stacks (FOWLER *et al.*, 1967). Detailed studies in emulsions (FOWLER *et al.*, 1970) and plastic detectors (PRICE *et al.*, 1971; O'SULLIVAN *et al.*, 1971) have shown that the heaviest cosmic rays are greatly enriched in r-process elements relative to the interstellar medium. Balloon observations of cosmic rays with $Z > 92$ have been reported (FOWLER *et al.*, 1970; PRICE *et al.*, 1971), but the uncertainty in their atomic number is large. Because of their rapid depletion by nuclear collisions and ionization loss, the mere presence of a finite flux of extremely

heavy ($Z > 82$) galactic cosmic ray nuclei at sub-relativistic energies (O'SULLIVAN *et al.*, 1971) suggests that they have traveled, on the average, for less than $\sim 10^5$ years. Since the shortest-lived nuclide whose decay products have been found (REYNOLDS, 1960) in solar system material, I^{129}, has a half-life of $\sim 2 \times 10^7$ years, the cosmic rays provide us with the possibility of detecting unstable elements with lifetimes between $\sim 10^5$ and $\sim 10^7$ years that cannot be detected in nature by other means. The observations of BHANDARI *et al.* (1971a, b) suggest that super-heavy elements have been made in nature with a half-life $> 10^7$ years. At this point one is reminded of the papers by DAKOWSKI (1969) and by ANDERS and HEYMANN (1969), who suggested that fission of a volatile super-heavy element with $112 \leqq Z \leqq 119$ (perhaps a longer-lived isotope of eka-mercury than MARINOV *et al.* claim to have made) may have been responsible for the excess neutron-rich Xe isotopes in certain meteorites, whose presence correlates with mercury and other volatiles.

With this long preamble on what may be one of the most exciting developments in the history of nuclear and cosmochemistry, we present our own observations.

OBERVATIONS

Using a solution consisting of $2HF:1H_2SO_4:4H_2O$ we have etched tracks in thin sections from the top cm of rock 12021 containing pigeonite crystals with dimensions of at least 1 mm. Figure 1 gives the distribution of track lengths measured thus far. These are minimum lengths since at least one end of the track is lost at a crystal surface. The atomic numbers we assign to the cosmic rays that left these tracks are thus minimum values. Figure 2 shows examples (a) of a stopping heavy nucleus and (b) of one of our longest tracks, which passes entirely through a 1 mm crystal.

Two observations support the assertion that these long etch features are tracks and not crystal dislocations or linear inclusions: (1) The angular distribution of all long

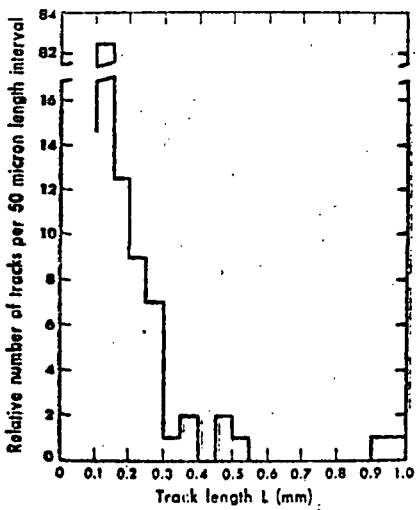

Fig. 1. Distribution of track lengths in rock 12021. Each length is a lower limit because the track extend beyond the edge of the crystal into the portion removed by grinding and polishing.

Fig. 2. Ultra-heavy cosmic rays in rock 12021. (a; top) A stopping nucleus with $Z \sim 65$. (b; middle and bottom) An energetic nucleus with $Z \sim 80$ passing through the entire thickness of a 1 mm wide pigeonite crystal. Six micrographs were lined up to make this photograph.

tracks, though peaked in a particular direction, is consistent with the expected distribution close to the surface of a rock and is not parallel to a low index crystallographic direction. (2) Annealing experiments show that Fe tracks disappear after one hour at 550°C, that most long tracks of high Z cosmic rays disappear after one hour at 630°C, and that fission fragment tracks disappear after one hour at 675°C. This behavior is consistent with the known fact that highly ionized regions anneal out at higher temperatures than do ionized region just above threshold (PERELYGIN *et al.*, 1969).

Kr^{84} Ion Calibration

In plastics (PRICE *et al.*, 1968a) and in glasses (FLEISCHER *et al.*, 1969) the etching rate along a track is a monotonic function of ionization rate and can be used to identify the energetic particle. In a crystalline solid a relationship between etching rate and ionization rate has not yet been established, partly because of the necessity to use beams of ions much heavier than have been available. However, assuming the entire portion of a particle's trajectory along which its ionization rate J exceeds a critical rate J_0 is revealed by chemical etching, one can calculate the maximum etchable length l_{max} as a function of Z if one knows the way in which J depends on Z and β. This calculation is of course invalid if the mineral has ever been heated enough to relax the damaged regions along the latent tracks.

From irradiation of minerals with Fe, Br, and I ions of ~ 70 MeV, PRICE *et al.* (1968b) deduced a relation between l_{max} and Z in which l_{max} ranges from ~ 8 μm for Fe to ~ 2 μm for U. Using a track-in-track method LAL *et al.* (1969) and LAL (1969) have obtained track length histograms of stopping Fe-group cosmic rays and have assigned values of l_{max} for Cr, Mn, and Fe of 5 μm, 8 μm, and 11.5 μm, assuming the most abundant species to be Fe. From these combined results we predicted that 10 MeV/N Kr^{84} ions have too low an ionization rate to leave etchable tracks. We find, however, that this is not the case. After an etching time such that tracks would have a diameter of ~ 1 μm, crystals of pigeonite, olivine and mica, as well as several glasses, record Kr^{84} ions of 10.35 MeV/N from the Berkeley Heavy Ion Accelerator with 100% efficiency. The etching rate appears to be independent of beam orientation within crystals and, surprisingly, the rate appears extremely insensitive to ionization rate. Whether the rate is diffusion-limited or reflects a true response that sharply increases at the critical ionization rate to a saturation value must be established by more detailed studies.

Additional calibrations with beams of Fe and heavier nuclei are badly needed, because the Kr results appear inconsistent with the assignment by LAL *et al.* (1969) of 11.5 μm to the etchable length of Fe tracks. The Kr results suggest that Fe should record over ~ 15 μm. Until this conflict is resolved, we continue to use the relation of PRICE *et al.* (1968b) but with the threshold ionization rate lowered such that Fe tracks have an etchable length of 11.5 μm.

Abundances of Cosmic Rays with $Z > 40$

Table 1 summarizes our charge distributions and compares the present day cosmic ray abundances, measured in balloon-borne detectors (FOWLER *et al.*, 1970; O'SULLIVAN *et al.*, 1971; PRICE *et al.*, 1971), with the abundances averaged over the surface

Table 1. Abundance of cosmic rays with $Z \geq 40$.

Charge group relative to Fe	Abundance if 12021 was at surface for 10^7 years	Abundance if 12021 was at 35 g/cm² for 3×10^8 y and at surface for 5×10^6 y‡	Present-day abundance (emulsions and plastics)
$\frac{Z \geq 40}{Fe}$	3.7×10^{-5}(76)*	7×10^{-5}(76)*	5.7×10^{-5}(139)*
$\frac{Z \geq 50}{Fe}$	6.9×10^{-6}(12)	2×10^{-5}(12)	3.2×10^{-5}(48)
$\frac{Z \geq 70}{Fe}$	1.3×10^{-6}(5)	8×10^{-6}(5)	1×10^{-5}(33)
$\frac{Z \geq 83}{Fe}$	5×10^{-7}(2)	5×10^{-6}(2)	3×10^{-6}(8)
$\frac{Z \geq 92}{Fe}$	†	?	1×10^{-6}(2)
$\frac{Z \geq 110}{Fe}$	†	?	$< 6 \times 10^{-7}$(0)

* Numbers of events are in parentheses.

† Relative abundances would equal 5×10^{-7} if the two 1 mm long tracks were made by cosmic rays with Z 92 or 110.

‡ All nuclei were assumed to have the same energy spectra in space. The greater energy loss rate and nuclear collision probability of the heavier nuclei were taken into account. The calculation is for 35 g/cm² burial beneath the surface of a semi-infinite body.

exposure time of rock 12021. Assuming all tracks were formed when the rock was on the very surface during 10^7 years gives the results in column 2. FLEISCHER *et al.* (1971) deduced a longer exposure time, $\sim 2.6 \times 10^7$ years, which would not seriously alter the results. Assuming half the tracks were formed at a depth of 35 g.cm² over a time of 3×10^8 years and half at the lunar surface gives the results in column 3. (MARTI and LUGMAIR (1971) have concluded from the abundances of Gd and Kr isotopes that rock 12021 was bombarded by cosmic rays for $\sim 3 \geq 10^8$ years while buried at ~ 35 g/cm². Our track density gradient at the surface of 12021 shows that it also was exposed at the surface for several million years).

Discussion

Although the detailed abundances are still uncertain, this work establishes that there has been a significant flux of ultra-heavy cosmic rays, with Z up to and beyond 80, over times of $\sim 10^7$ to $\sim 10^8$ years. The overall abundance pattern over this period appears to be similar to that obtained in current balloon flights for the present-day flux, but we cannot claim that this similarity has been established until better calibrations in minerals are available.

If the two longest tracks were made by elements with $Z \geq 110$, the flux of such super-heavy cosmic rays could be as high as 1/m² year, which is $\sim 5 \times 10^{-7}$ times the Fe flux. This flux would be detectable in the present-day cosmic radiation after a long exposure in an orbiting laboratory or in a series of balloon exposures of plastics and emulsions of large area. In view of the work of MARINOV *et al.* (1971) and of BHANDARI *et al.* (1971a, b), further studies of long tracks in moon rocks and an increased effort in long, high altitude exposures would be extremely important.

The possibility that our charge distribution might be distorted because the heaviest cosmic rays were preferentially attenuated in a long subsurface exposure of rock 12021 was pointed out to us at the Apollo 12 conference by R. M. WALKER. To avoid this possible distortion in the future, we have requested samples of 12004, which has large pigeonite crystals and whose short Kr^{81}/Kr^{83} exposure age (BOCHSLER *et al.*, 1971) makes it more suitable than 12021 for our work.

The ionization rate of a hypothetical magnetic monopole is essentially constant and such a particle would leave a track with the same etching rate all along its length, which might even be as long as several meters. Our Kr results show that a track with a constant etch rate along its length was not necessarily produced by a monopole but could have been produced by a heavy nucleus. Assuming, however, that both of our 1 mm long tracks were made by monopoles, we arrive at an upper limit of $\sim 3 \times 10^{-8}/cm^2$ year on the flux of monopoles with magnetic charge $g \geq 3\hbar c/2e$. This flux is based on the total cosmic ray exposure age of $\sim 3 \times 10^8$ years obtained by MARTI and LUGMAIR (1971). Previous limits on the flux of *primary* monopoles in the universe are far lower than this, $\sim 10^{-14}/cm^2$ year (OSBORNE, 1970; FLEISCHER *et al.*, 1970). However, our limit is highly significant for *secondary* monopoles that might have been produced by high energy gamma rays resulting from cosmic ray interactions in the moon. The implications of this result will be discussed in detail in a separate publication, where we emphasize that the production of monopole pairs by high energy gamma rays should be more readily detectable in the moon than in the earth.

The fact that 10.35 MeV/N Kr ions leave etchable tracks in minerals may raise questions concerning the interpretation of the exciting observations of BHANDARI *et al.* (1971a, b), who identify extinct super-heavy elements by the presence of tracks longer than fission tracks of U^{238} and Pu^{244} and longer than slowing Fe nuclei would be expected to leave. Without detracting from their important work, we simply emphasize that with any reasonable ionization equation we conclude from the Kr results that Fe ought to record over at least 15 μm.

Acknowledgments—We are grateful to A. Ghiorso for arranging for the 10 MeV/N irradiations. We are indebted to R. Cowsik, R. L. Fleischer, R. M. Walker, A. Ghiorso, and S. G. Thompson for useful discussions and to NASA, the Atomic Energy Commission, and the National Science Foundation for financial support.

REFERENCES

ANDERS E. and HEYMANN D. (1969). Elements 112 to 119: Were they present in meteorites? *Science* **164**, 821–822.

BARBER D. J., HUTCHEON I., PRICE P. B., RAJAN R. S., and WENK H. R. (1971). Exotic particle tracks and lunar history. Second Lunar Science Conference (unpublished proceedings).

BHANDARI N., BHAT S. G., LAL D., RAJAGOPALAN G., TAMHANE A. S., and VENKATAVARADAN V. S. (1971a). Evidence for the existence of super-heavy elements in extraterrestrial samples, *Nature* (to be published).

BHANDARI N., BHAT S. G., LAL D., RAJAGOPALAN G., TAMHANE A. S., and VENKATAVARADAN V. S. (1971b). The spontaneous fission record of uranium and extinct transuranci elements in Apollo 12 samples. Second Lunar Science Conference (unpublished proceedings).

BOCHSLER P., EBERHARDT P., GEISS J., GRAF N., GROGLER N., KRAHENBUHL V., MORGELI M., SCHWALLER H., and STETTLER A. (1971). Potassium argon ages, exposure ages and radiation history of lunar rocks. Second Lunar Science Conference (unpublished proceedings).

DAKOWSKI M. (1969). The possibility of extinct super-heavy elements occurring in meteorites. *Earth and Plan. Sci. Lett.* **6**, 152–154.

FLEISCHER R. L., PRICE P. B., WALKER R. M., MAURETTE M., and MORGAN G. (1967). Tracks in heavy primary cosmic rays in meteorites. *J. Geophys. Res.* **72**, 355–366.

FLEISCHER R. L., PRICE P. B., and WOODS R. T. (1969). Nuclear-particle-track identification in inorganic solids. *Phys. Rev.* **188**, 563–567.

FLEISCHER R. L., HART, H. R. JR., JACOBS I. S., PRICE P. B., SCHWARZ W. M., and WOODS R. J. (1970). Magnetic monopoles: Where are they and where aren't they? *J. of Appl. Phys.* **41**, 958–965.

FLEISCHER R. L., HART, H. R. JR., COMSTOCK G. M., and EVWARAYE (1971). The particle track record of the ocean of storms. Second Lunar Science Conference (unpublished proceedings).

FOWLER P. H., ADAMS R. A., COWEN V. G., and KIDD J. M. (1967). The charge spectrum of very heavy cosmic ray nuclei. *Proc. Roy. Soc.* **A301**, 39–45.

FOWLER P. H., CLAPHAM V. W., COWEN V. G., KIDD J. M., and MOSES R. T. (1970). The Charge spectrum of very heavy cosmic ray nuclei. *Proc. Roy. Soc.* **A318**, 1–43.

LAL D., RAJAN R. S., and TAMHANE A. S. (1969). On the study of the chemical composition of nuclei of $Z > 22$ in the cosmic radiation using meteoritic minerals as detectors. *Nature* **221**, 33–37.

LAL D. (1969). Recent advances in the study of fossil tracks in meteorites due to heavy nuclei of cosmic radiation. *Space Sci. Rev.* **9**, 623–650.

MARINOV A., BATTY C. J., KILVINGTON A. I., and HEMINGWAY J. D. (1971). Evidence for the possible existence of a superheavy element with atomic number 112. *Nature* **229**, 464–467.

MARTI K. and LUGMAIR G. W. (1971). Kr^{81}–Kr and K–Ar^{40} ages, cosmic ray spallation products and neutron effects in Apollo 11 and 12 lunar samples. Second Lunar Science Conference (unpublished proceedings).

OSBORNE W. Z. (1970). Limits on magnetic monopole fluxes in the primary cosmic radiation from inverse Compton scattering and muon poor extensive air showers. *Phys. Rev. Lett.* **24**, 1441–1445.

OSULLIVAN D., PRICE P. B., SHIRK E. K., FOWLER P. H., KIDD J. M., KOBETICH E. J., and THORNE R. (1971). High resolution measurements of slowing cosmic rays from Fe to U. *Phys. Rev. Lett.* **26**, 463–466.

PERELYGIN V. P., SHADIEVA N. H., TRETIAKOVA S. P., BOOS A. H., and BRANDT R. (1969). Ternary fission produced in Au, Bi, Th, and U with Ar ions. *Nucl. Phys.* **A127**, 577–585.

PRICE P. B., FLEISCHER R. L., PETERSON D. D., O'CEILAIGH C., O'SULLIVAN D., and THOMPSON A. (1968a). High resolution study of low-energy heavy cosmic rays with lexan track detectors. *Phys. Rev. Lett.* **21**, 630–633.

PRICE P. B., FLEISCHER R. L., and MOAK C. D. (1968b). On the identification of very heavy cosmic ray tracks in meteorites. *Phys Rev.* **167**, 277–282.

PRICE P. B., FOWLER P. H., KIDD J. M., KOBETICH E. J., FLEISCHER R. L., and NICHOLS G. E. (1971). Study of the charge spectrum of extremely heavy cosmic rays using combined plastic detectors and nuclear emulsions. *Phys. Rev.*, in press.

REYNOLDS J. (1960). Determination of the ages of elements. *Phys. Rev. Lett.* **4**, 8–10.

(4)

Proceedings of the Second Lunar Science Conference, Vol. 3. pp. [redacted]
The M.I.T. Press

Solar flares, the lunar surface, and gas-rich meteorites

D. BARBER,† R. COWSIK‡, I. HUTCHEON, P PRICE, and R. RAJAN
Department of Physics, University of California, Berkeley, California 94720

(*Received* 22 *February* 1971; *accepted in revised form* 30 *March* 1971)

Abstract—An updated interplanetary energy spectrum of Fe nuclei from solar flares, based on tracks in the Surveyor III glass filter, is presented. From that spectrum and the track density profile in rock 12022, the average rock erosion rate over 10^7 years is estimated to be ~ 3 Å/year. This rate is $\sim$ three times higher than our initial estimate and is consistent with the rate inferred by HÖRZ *et al.* from microcratering studies of 12022 and several other rocks. Track densities of $\sim 10^{10}$ to 10^{11}/cm^2 are quite common in the finest component of the soil at all depths down to at least 60 cm and have also been observed for the first time in interior grains of gas-rich meteorites. Erosion mechanisms and the origin of the lunar and meteoritic grains with high track densities are discussed.

INTRODUCTION

HIGH TRACK DENSITIES and steep track density gradients have been observed in interior grains of certain gas-rich meteorites (LAL and RAJAN, 1969; PELLAS *et al.*, 1969), in the top mm of lunar rocks and in crystals and glass from the lunar soil (CROZAZ *et al.*, 1970; FLEISCHER *et al.*, 1970; LAL *et al.*, 1970; PRICE and O'SULLIVAN, 1970; BORG *et al.*, 1970; BARBER *et al.*, 1971). The tracks were almost certainly produced by heavy nuclei ($Z \approx 26$) emitted in solar flares with a steeply falling energy spectrum. Heavy nuclei in the galactic cosmic rays have an energy spectrum that rises less steeply at low energies than does the solar particle spectrum but that penetrates much more deeply, down to several cm. The presence of tracks of solar origin in isolated interior grains were compacted into meteorites and that the peak shock pressure during compaction did not exceed ~ 100 kilobars, the value below which tracks made visible by chemical etching are not erased (AHRENS *et al.*, 1970). The presence of solar tracks in sub-surface lunar soil demands that those layers were once exposed at the surface.

If the rock surface was being eroded during its irradiation or was separated from the source of energetic particles by either solid or gaseous matter, the observed track density gradient would be lower than the predicted gradient (PRICE *et al.*, 1967). Until now the use of this concept to infer erosion rates and irradiation history has been impeded by ignorance of the average interplanetary energy spectrum of Fe-group nuclei ($Z \approx 26$).

Three recent developments make it profitable for us to re-examine lunar erosion, ancient solar flares, and the history of the lunar soil and gas-rich meteorites: (1) techniques for observing track densities up to $\sim 5 \times 10^{11}$/cm^2 with high voltage

† Present address: Department of Physics, Essex University, Colchester, U.K.
‡ On leave from Tata Institute of Fundamental Research, Bombay, India.

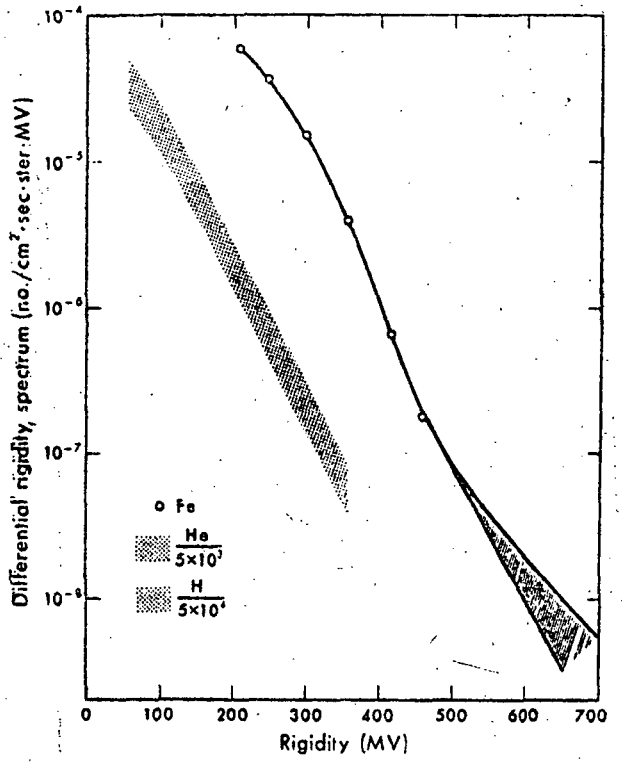

Fig. 1. The observed tracks in Surveyor glass are assumed to be solely due to Fe ions, and the rigidity spectrum is derived, using observed variation with depth. The hatched region at large rigidities represents uncertainty due to a background of fission tracks. The expected curve, with an indicated uncertainty factor of 2, was computed on the basis of satellite measurements of solar protons and alphas, using the proper photospheric abundance ratios. This predicted curve falls much below the observed curve, indicating enhanced emission of Fe-group nuclei.

electron microscopy; (2) direct measurement of the gradient of Fe tracks in glass from the Surveyor III camera after a 2.6 year exposure to solar flares during 1967–69; (3) calibration of the glass and of lunar minerals with beams of 10.3 MeV/N Ar^{40} and Kr^{84} ions.

ENERGY SPECTRUM OF INTERPLANETARY FE NUCLEI

Three groups have measured the track density from interplanetary Fe-group nuclei as a function of depth in portions of the flint glass lens filter that was exposed on the lunar surface from May 20, 1967 until the Apollo 12 astronauts brought the Surveyor 3 camera back to earth in November, 1969 (PRICE *et al.*, 1971; CROZAZ and WALKER, 1971; FLEISCHER *et al.*, 1971). We have critically compared the available data and in Fig. 1 we present a revised differential rigidity spectrum for that 2.6 year period that takes into account several factors not previously considered by all three groups: (1) Using beams of Ar^{40} and Kr^{84} ions, we have determined the dependence

of cone angles of etched tracks in the glass on ionization rate. On the basis of this we estimate that the track of an Fe ion can be recognized between 2 and 35 microns of its residual range. (2) We have calculated an accurate range-energy relation for the composition of the flint glass. (3) FLEISCHER *et al.* (1971) have shown that there is a uniform background of cosmic-ray induced fission of lead atoms in the glass that distorts the highest energy portion of the spectrum. (4) Neil Nickle (private communication) has provided us with a recently measured size distribution of lunar dust particles on the glass surface that distorts the lowest energy portion of the spectrum. We have taken into account the degrading effect of these dust grains, which are discontinuously distributed and allow some of the lowest energy particles to reach the glass without energy loss. The remaining, main source of uncertainty in the new spectrum is the human efficiency for observing etched tracks with various cone angles inclined at various angles to the glass surface. Very close to the filter's surface we measured, using optical and scanning electron microscopy, a track density of $1.5 \times 10^6/\text{cm}^2$ ster. The values obtained by the two methods were selfconsistent and agree with the value by CROZAZ *et al.* (1971). Deeper in the glass we use the data of FLEISCHER *et al.* (1971), who have a high efficiency for the observation of tracks, since they scan a surface which is normal to the mean direction of the flux of the Fe ions.

In our recent paper (PRICE *et al.*, 1971) we pointed out that the flux of Fe nuclei in Fig. 1 is far greater than expected on the assumption that the sun emits energetic particles in the ratio of their photospheric abundances. In drawing this conclusion we have used the published satellite data for solar alpha particles and protons of LANZEROTTI (1969–70) and the proton data of BOSTROM *et al.* (1968–70) and of HSIEH and SIMPSON (1971). In the energy interval where they overlap, the spectra of these three groups agree reasonably well for most flares, with the data of Hsieh and Simpson being low by as much as a factor 2 for the April 12, 1969 flare. The agreement with the solar proton spectra inferred by FINKEL *et al.* (1971) from radiochemical measurements on Co^{56} and Mn^{54} in rock 12002 is fair, tending to be low by up to a factor 2 (J. R. ARNOLD, private communication).

As an illustration of the enhancement of Fe flux, the broad curve in Fig. 1 shows the predicted Fe rigidity spectrum given by the product of the alpha particle spectrum of Lanzerotti and the solar abundance ratio $(\text{Fe/He})_\odot \approx 2 \times 10^{-4}$ calculated by Ross (1970) from the recent solar Fe abundance deduced by WOLNIK *et al.* (1970). We have attributed the difference between the observed and predicted flux to the preferential leakage of low energy Fe nuclei from the accelerating region because of their incomplete ionization and consequent high magnetic rigidity (PRICE *et al.*, 1971). Our present analysis places this observation of a heavy ion enhancement on an even firmer basis than before. The enhancement is far greater than the maximum uncertainty in solar proton spectrum based on satellite and radiochemical data.

In the remainder of this paper we assume that the spectrum in Fig. 1 represents the flux level during the active half of an 11 year solar cycle and that the flux drops to zero during the inactive half, so that in 10^6 years the accumulated number of Fe tracks would be $(10^6 \times 3.2 \times 10^7 \text{ sec/y})/5.5$ times higher, assuming that the intensity of the present solar cycle is equal to the average intensity over millions of years.

LUNAR EROSION RATE

The method of determining rock erosion rate depends on a comparison of track density gradients in a rock and in the Surveyor glass and is completely independent of the ratio of Fe ions to protons in solar flares.

The track density gradient in a lunar rock is most reliably obtained from measurements on an etched, polished section rather than on individual grains removed from various locations. Figure 2 shows the track density profile taken in a region of rock 12022 that contains no impact pits. This is a particularly valuable rock because of its simple history; in contrast to 10017 (PRICE and O'SULLIVAN, 1970; CROZAZ *et al.*, 1970; FLEISCHER *et al.*, 1970) and 12063 (CROZAZ *et al.*, 1971), rock 12022 was irradiated only from one direction and appears not to have received a sub-surface exposure. Our measurements, which combine transmission electron microscopy and optical microscopy, cover four orders of magnitude of depth and extend from track densities of $\sim 3 \times 10^6/\text{cm}^2$ up to $\sim 6 \times 10^9/\text{cm}^2$ at a depth of ~ 3 μm below the surface.

From the profile deep inside the rock, due to galactic Fe-group nuclei, we infer a surface residence time of $\sim 1 \times 10^7$ years. In Fig. 2 we show the expected track

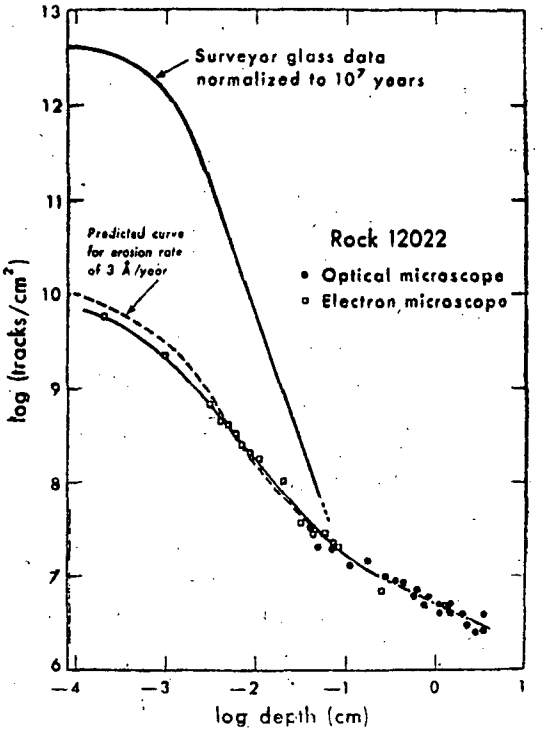

Fig. 2. The solar contribution to track densities during 10^7 years is estimated by assuming that the observed track densities in Surveyor glass represented the contribution over one-half of an 11-year solar cycle. On the basis of this and assuming a uniform erosion rate of 3 Å/year, the track density gradient predicted for a lunar rock is in good agreement with that measured for rock 12022.

densities at various depths deduced (making the aforementioned assumptions) from the measurements on the Surveyor glass filter. This dashed curve was derived assuming a mean erosion rate of 3 Å/year and is in excellent agreement with the measured track densities in rock 12022. The erosion rate of $\sim$ 3 Å/year is reliable only to the extent that the spectrum in Fig. 1 truly represents the average solar flare spectrum over 10^7 years. From their radiochemical study of 12002, FINKEL *et al.* (1971) conclude that the proton intensity in the present solar cycle is representative of the average over $\sim 10^6$ years. Thus, $\sim$ 3 Å/year appears to be a reasonable average value for recent lunar history, but of course may not be representative of erosional processes at an earlier epoch. For example, to build up a regolith $\sim$ 7 meters thick at Oceanus Procellarum (SHOEMAKER and HAIT, 1971) in 3.3×10^9 years (ALBEE *et al.*, 1971) would necessitate an *average* erosion rate of $\sim$ 20 Å/year if the regolith were derived from comminution of local rock. We emphasize that these two rates are not incompatible if they apply to quite different epochs or if the regolith is built up dominantly by large meteorite collisions that would destroy rocks of the size brought back to earth.

At least three processes are responsible for the erosion of rock: (1) Sputtering of individual atoms by the solar wind (mainly hydrogen) may remove as much as 0.4 Å/year (WEHNER *et al.*, 1963), depending on the average angle of inclination of the rock surface of the sun. (2) The flux of heavy nuclei emitted in solar flares is sufficiently great (Fig. 1) that, in the absence of other erosional processes, the outer 10 μm of rock would accumulate $\sim 10^{12}$ Fe-group tracks in a million years, as well as a considerably larger density of more lightly damaged regions produced by ions of abundant elements like C, O, Ne, Mg, Si, and S. At a dose of $\sim 10^{13}$/cm^2 At ions certain minerals develop extensive strains and fractures in regions where the ions have stopped (SEITZ *et al.*, 1970), so that excessively radiation-damaged layers might flake off and contribute to the regolith. We estimate that the erosion rate by this mechanism might reach 0.1 or 0.2 Å/year for feldspars and certain other minerals that are especially susceptible to radiation damage. If however, sputtering removes as much as 0.4 Å/year, the density of solar flare tracks would be limited to $\sim 10^{11}$/cm^2 and flaking would probably not occur. (3) Micrometeorites certainly contribute to rock erosion. The magnitude of their contribution is uncertain because of uncertainty in the present-day flux of micrometeorites (known to within no better than $\pm 3\times$) and in the longtime constancy of the flux. In a very careful study of microcraters on lunar rocks, HÖRZ *et al.* (1971) arrive at an average erosion rate of $\sim$ 1 to 2 Å/year and a surface lifetime of $\sim 10^7$ years before destruction by a large micrometeorite, subject to the above uncertainties. It is not clear from microscopic observations alone whether the crater distributions on Apollo 12 rocks have reached a steady state or not, but in order to account for the 3 Å/year inferred for rock 12022, microcratering must be a more important mechanism than sputtering, which cannot remove more than $\sim$ 0.4 Å/year.

At the Apollo 12 conference we estimated the erosion rate of 12022 to be no more than 1 Å/year; FLEISCHER *et al.* (1971) quoted a rate of 0 to 2 Å/year in their analysis of track gradients reported by several groups at the Apollo 11 conference; and CROZAZ and WALKER (1971) quoted a value of $\sim$ 10 Å/year, based on an apparent erosion

equilibrium for the track gradient in 12063. The agreement between our revised value of ~ 3 Å/year for 12022 and the rate of 1 to 2 Å/year arrived at by HÖRZ *et al.* (1971) is sufficiently close that one can conclude that the micrometeorite flux over the last 10^7 years must have been fairly similar to the present-day rate, on which they based their calculations.

The effects of erosion undoubtedly depend to some extent on the size of the body being eroded and must be taken into account in attempting to understand the origin of the lunar fines and of the highly irradiated grains in gas-rich meteorites as well. Atomic sputtering should be essentially independent of the size of the body. Micrometeorite bombardments will not affect track gradients in submillimeter particles because none of these particles will survive a single collision. The only fine particles available for study are those that have avoided collision.

To summarize, track gradients in small particles are less steep than that predicted from the energy spectrum observed in the Surveyor glass. This discrepancy could arise from sputtering-type erosion or from coverage by a layer of matter but probably not from erosion by radiation-induced cracking. Micrometeorite bombardment erodes large particles and rocks but simply destroys small particles. This discussion is pertinent to the section that follows.

HIGHLY IRRADIATED GRAINS IN THE REGOLITH AND IN GAS-RICH METEORITES

Any features common to both the moon and the meteorites contribute to our understanding of the origin of both. For example, the chemical composition and mineralogy of many of the lunar rocks are similar to those of eucrites (WÄNKE *et al.*, 1970). GANAPATHY *et al.* (1970a, b) conclude from an analysis of enriched concentrations of certain trace elements that 2% of the lunar soil is of carbonaceous chondritic origin, presumably from accumulated infall. The enrichment is most pronounced in the small grain size fraction.

Using a 1 MeV electron microscope, BORG *et al.* (1970) and DRAN *et al.* (1970) have found extremely high track densities ($>10^{11}$/cm^2) in a large fraction of the finest grains in the lunar soil but have failed to find any tracks in grains taken from gas-rich meteorites. They have emphasized the differences in habit and texture features of lunar and meteoritic grains. Their inability to etch the tracks in the lunar grains and the predominance of high track densities in the *smallest* grains led them to suggest that solar suprathermal heavy ions, with damage rates below the threshold for etching, were responsible for the tracks. Suprathermal protons at high flux levels have been observed on several occasions by FRANK (1970).

With a 650 kev electron microscope we have found extremely high densities of etchable tracks at all depths down to 60 cm in fines from Apollo cores (BARBER *et al.*, 1971) as well as in thin sections of the Kapoeta and Fayetteville gas-rich meteorites. From both etching and dark field work we deduce that $\sim 20\%$ of fines < 5 μm dia have track densities $>10^{10}$/cm^2. In Fayetteville about 5–10% of the smaller grains have $\sim 10^{10}$ tracks/cm^2. Micrographs of unetched tracks in a particle of lunar soil and in the Fayetteville meteorite are presented in Fig. 3. Although the meteorite studies are still at a preliminary stage, our observations of track densities comparable

to those in lunar grains and at least 20 times greater than had been originally reported in track-rich meteorite grains (LAL and RAJAN, 1969; PELLAS *et al.*, 1969) are highly significant because they remove one of the previous major distinctions (BORG *et al.*, 1970) between lunar grains and meteoritic grains and suggest the possibility of a similar origin. Track densities of $2 \times 10^{10}/cm^2$ or higher are present in the interior of crystals more than 10 μm diameter within sections of the Fayetteville meteorite which were thinned by ion-beam machining. Similar high track densities also exist in smaller (< 0.5 μm diameter) euhedral crystals. In previous optical microscope and scanning electron microscope studies of etched grains of gas-rich meteorites those grains with track densities exceeding $10^{10}/cm^2$ were never noticed because they completely dissolved in the standard etching process. The tracks in meteorites have been mainly studied by diffraction contrast imaging (i.e., without etching); the absence of the amorphous layer present on lunar grains makes etching less beneficial (BARBER *et al.*, 1971) in seeing tracks. And etching the meteorites is disadvantageous because it can cause grains which are barely held within the thinned and weakened fabric to drop out. We have established, however, that the tracks in most lunar and meteoritic minerals are etchable, under suitable conditions.

If radiation-induced flaking is a more important erosional process than is sputtering, we might be able to attribute the track-rich grains in the lunar soil to flaked-off surface layers of rocks. We believe, however, that there are difficulties with this simple picture. The surfaces of rocks show no evidence of extreme stress nor do they contain track densities as high as $10^{10}/cm^2$. The majority of the track-rich grains, both in the lunar soil and in the meteorites (Fig. 3), exhibit rather nice electron diffraction patterns that argue against extreme radiation damage. Admittedly, many of the fines have amorphous outer layers (thickness $\sim$ 500 Å) attributed to accumulated damage by solar wind bombardment but the interiors are still crystalline, (Fig. 3(a)). These findings are in agreement with the work of DRAN *et al.* (1970) and BORG *et al.* (1970), who emphasized that the grains were not disordered. The observed euhedral habits of some of the meteoritic track-rich grains also argue against radiation stress-induced fracture. In the Kapoeta meteorite, however, electron microscopy reveals that many of the small grains contain minute cracks and microstructural features are severely distorted. The electron diffraction patterns correspondingly exhibit arcs and extended spots. So far we have failed to see tracks in the carbonaceous chondrites, Murray and Orgeuil, and other observations we have made suggest that tracks will not be found.

We have recently suggested that some of the highly irradiated lunar grains are fragments of infallen extra-lunar dust (BARBER *et al.*, 1971). It has previously been suggested that some of the gas-rich meteorites were assembled by sintering of circumsolar grains (LAL and RAJAN, 1969; PELLAS *et al.*, 1969). Continuing observations of ion-beam-thinned sections of gas-rich meteorites should provide severe constraints on their mode of origin. It would be especially useful to find a large grain with a high track density and a gradient that could be related to an erosional process.

We regard it as highly unlikely that suprathermal heavy ions were responsible for the observed high track densities. A suprathermal ion energy spectrum should continue to rise to a peak at low energy, so that the track length distribution should

Fig. 3. (a) Dark field electron micrograph (650 KeV) of tracks of solar flare particles in a grain from the Apollo 12 lunar fines. Bar mark 0.5 μm. (b) Dark field electron micrograph (650 KeV) of fossil particle tracks in a section of the Fayetteville meteorite which was thinned by sputter-etching with 5 KeV argon ions. Bar mark 0.5 μm.

be peaked at short lengths. Our electron microscope observations of both etched and unetched tracks show that the track length distribution on lunar grains ≥ 10 μm thinned by sputter-etching is not peaked at short length and is typical of randomly oriented tracks that penetrate the entire grain.

Acknowledgments—We are indebted to A. GHIORSO for the Ar and Kr ion irradiations, to N. NICKLE and D. ROBERTSON for help with the Surveyor glass, to K. C. HSIEH, J. D. SULLIVAN, C. O. BOSTROM, L. J. LANZEROTTI, J. R. ARNOLD, and R. C. REEDY for helpful discussions and data on solar protons and alpha particles, and to NASA and the National Science Foundation for financial support.

REFERENCES

AHRENS T. J., FLEISCHER R. L., PRICE P. B., and WOODS R. T. (1970). Erasure of fission tracks in glasses and silicates by shock waves, *Earth Planet. Sci. Lett.* **8**, 420–426.

ALBEE A. L., BURNETT D. S., CHODOS A. A., HAINES E. L., HUNEKE J. C., PAPANASTASSIOU D. A., PODOSEK F. A., RUSS G. P., TERA F., and WASSERBURG G. J. (1971) Rb-Sr Ages, chemical abundance patterns and history of lunar rocks. Second Lunar Science Conference (unpublished proceedings).

BARBER D. J., HUTCHEON I., and PRICE P. B. (1971) Extralunar dust in Apollo cores? *Science* **171**, 372–374.

BORG J., DRAN J. C., DURRIEU L., JOURET C., and MAURETTE M. (1970) High voltage electron microscope studies of fossil nuclear particle tracks in extra-terrestrial matter. *Earth Planet. Sci. Lett.* **8**, 379–386.

BOSTROM C. O., WILLIAMS D. J., and ARENS J. F. (1968–70) Solar proton monitoring. Unpublished data in ESSA Solar-Geophysical Data Bulletins.

CROZAZ G. and WALKER R. M. (1971) Solar particle tracks in glass from the Surveyor 3 spacecraft. *Science*, to be published.

CROZAZ G., WALKER R., and WOOLUM D. (1971) Cosmic ray studies of "recent" dynamic processes. Second Lunar Science Conference (unpublished proceedings).

CROZAZ G., HAACK U., HAIR M., MAURETTE M., WALKER R., and WOOLUM D. (1970) Nuclear track studies of ancient solar radiations and dynamic lunar processes. *Proc. Apollo 11 Lunar Sci. Conf., Geochim. Cosmochim. Acta* Suppl. 1, Vol. 3, pp. 2051–2070. Pergamon.

DRAN J. C., DURRIEU L., JOURET C., and MAURETTE M. (1970) Habit and texture studies of lunar and meteoritic materials with a 1 MeV electron microscope. *Earth Planet. Sci. Lett.* **9**, 391–400.

FINKEL R. C., ARNOLD J. R., REEDY R. C., FRUCHTER J. S., LOOSLI H. H., EVANS J. C., SHEDLOVSKY J. P., IMAMURA M., and DELANY A. C. (1971) Depth Variation of cosmogenic nuclides in a lunar surface rock. Second Lunar Science Conference (unpublished proceedings).

FLEISCHER R. L., HAINES E. L., HART H. R., WOODS R. T., and COMSTOCK G. M. (1970) The particle track record of the Sea of Tranquility. *Proc. Apollo 11 Lunar Sci. Conf., Geochim. Cosmochim. Acta* Suppl. 1, Vol. 3, pp. 2103–2120. Pergamon.

FLEISCHER R. L., HART H. R., and COMSTOCK G. M. (1971) Very heavy solar cosmic rays: Energy spectrum and implications for lunar erosion. *Science*, to be published.

FRANK L. A. (1970) On the presence of low energy protons ($5 \leq E \leq 50$ keV) in the interplanetary medium. *J. Geophys. Res.* **75**, 707–716.

GANAPATHY R., KEAYS R. R., LAUL J. C., and ANDERS E. (1970a) Trace elements in Apollo 11 lunar rocks: implications for meteorite influx and origin of moon. *Proc. Apollo Lunar Sci. Conf., Geochim. Cosmochim. Acta* Suppl. 1, Vol. 2, pp. 1117–1142. Pergamon.

GANAPATHY R., KEAYS R. R., and ANDERS E. (1970b) Apollo 12 Lunar samples: trace element analysis of a core and the uniformity of the regolith. *Science*, in press.

HORZ F., HARTUNG J. B., and GAULT D. E. (1971) Lunar microcraters. Second Lunar Science Conference (unpublished proceedings).

HSIEH K. C. and SIMPSON J. A. Private communication of unpublished results.

LAL D., MACDOUGALL D., WILKENING L., and ARRHENIUS G. (1970) Mixing of the lunar regolith and cosmic ray spectra: Evidence from particle-track studies. *Proc. Apollo 11 Lunar Sci. Conf., Geochim. Cosmochim. Acta* Suppl. 1, Vol. 3, pp. 2295–2303. Pergamon.

LAL D. and RAJAN R. S. (1969) Observations relating to space irradiation of individual crystals of gas-rich meteorites. *Nature* **223**, 269–271.

LANZEROTTI L. J. (1969–70) Unpublished data in World Data Center Reports.

PELLAS P., POUPEAU G., LORIN J. C., REEVES H., and AUDOUZE J. (1969) Primitive low-energy particle irradiation of meteoritic crystals. *Nature* **223**, 272–274.

PRICE P. B. and O'SULLIVAN D. (1970) Lunar erosion rate and solar flare paleontology. *Proc. Apollo 11 Lunar Sci. Conf., Geochim. Cosmochim. Acta* Suppl. 1, Vol. 3, pp. 2351–2359. Pergamon.

PRICE P. B., HUTCHEON I., COWSIK R., and BARBER D. J. (1971) Enhanced emission of iron nuclei in solar flares. *Phys. Rev. Lett.* to be published.

PRICE P. B., RAJAN R. S., and TAMHANE A. S. (1967) On the preatmospheric size and maximum space erosion rate of the Patwar stony-iron meteorite. *J. Geophys. Res.* **72**, 1377–1388.

ROSS J. E. (1970) Abundance of iron in the solar photosphere. *Nature* **225**, 610–611.

SEITZ M., WITTELS M. C., MAURETTE M., and WALKER R. M. (1970) Accelerator irradiations of minerals: implications for track formation mechanisms and for studies of lunar and meteoritic minerals. *Rad. Effects* **5**, 143–148.

SHOEMAKER E. M. and HAIT M. H. (1971) The bombardment of the lunar maria. Second Lunar Science Conference (unpublished proceedings).

WÄNKE H., RIEDER R., BADDENHAUSEN H., SPETTEL B., TESCHKE F., QUIJANO-RICO M., and BALACESCU A. (1970) Major and trace elements in lunar material. Proc. *Apollo* 11 *Lunar Sci. Conf.*, *Geochim. Cosmochim. Acta* Suppl. 1, Vol. 2, pp. 1719–1727. Pergamon.

WEHNER G. K., KENKNIGHT C., and ROSENBERG D. L. (1963) Sputtering rates under solar-wind bombardment. *Planet. Space Sci.* **11**, pp. 885–895.

WOLNIK S. J., BERTHEL R. O., and WARES G. W. (1970) Shock-tube measurements of absolute gf-values for FeI. *Astrophys. J.* **162**, 1037–1047.

Proceedings of the Second Lunar Science Conference, Vol. 1, pp. 000–000.
Copyright © 1971 by The M.I.T. Press.

Lunar bytownite from sample 12032,44

H.-R. WENK and G. L. NORD
Department of Geology and Geophysics, University of California at Berkeley
Berkeley, California 94720

(*Received* 18 *February* 1971; *accepted in revised form* 22 *February* 1971)

Abstract—Optical U-stage measurements, chemical microprobe data, and X-ray precession photographs of a bytownite twin group from rock 12032,44 are compared. Sharp but weak b and no c-reflections were observed for this An89 bytownite indicating a partly disordered structure. Euler angles, used to characterize the orientation of the optical indicatrix, compare better with values for plutonic than for volcanic plagioclase. This indicates that structural and optical properties cannot be directly correlated.

INTRODUCTION

THIS PAPER REPORTS optical, chemical, and structural data for a group of plagioclase crystals twinned after various laws. The group of crystals was a fragment in the fines of specimen 12032,44 from Oceanus Procellarum. Rock 12032,44 belongs to WOOD's (1971) group of gabbroic anorthosites or norites which may come from the lunar highlands. A thin section, prepared from the specimen, which is 2 mm in size (Fig. 1a), was cut perpendicular to [100] in order to facilitate measurements of twin lamellae and cleavage. Optical measurements were obtained on a Leitz U-stage for locations indicated in Fig. 1a. The section was then polished and chemical analyses were done using an ARL microprobe. Finally, two crystal fragments (X and R in Fig. 1a) were picked from the thin section for X-ray analysis on a precession camera (X) and for determination of the refractive index on a spindle stage (E). All measurements were made on the same group of crystals and are therefore directly comparable.

CHEMICAL COMPOSITION

As both structure and optical properties of plagioclase are sensitive to variations in chemical composition and conditions during the formation of the crystal, it is essential to have accurate chemical analyses; 77 spot analyses have been done over the whole group of crystals. Representative results are shown in Fig. 1b and Table 1. The plagioclase is a bytownite, An 85–90, the rim slightly more sodic than the center. Fe is the only other element which we have found to be relatively abundant. It is assumed to be in the ferrous oxidation state and evidence from Mössbauer spectra indicates that it occurs both in the tetrahedral and calcium sites (APPLEMAN *et al.*, 1971; HAFNER and VIRGO, 1971).

OPTICAL ANALYSIS

The crystals shown in Fig. 1a form a multiple twin group. They appear undeformed but the composition planes are slightly curved. U-stage measurements with a Leitz UM3 20X objective have been done in areas A and B of the specimen (Fig. 1a).

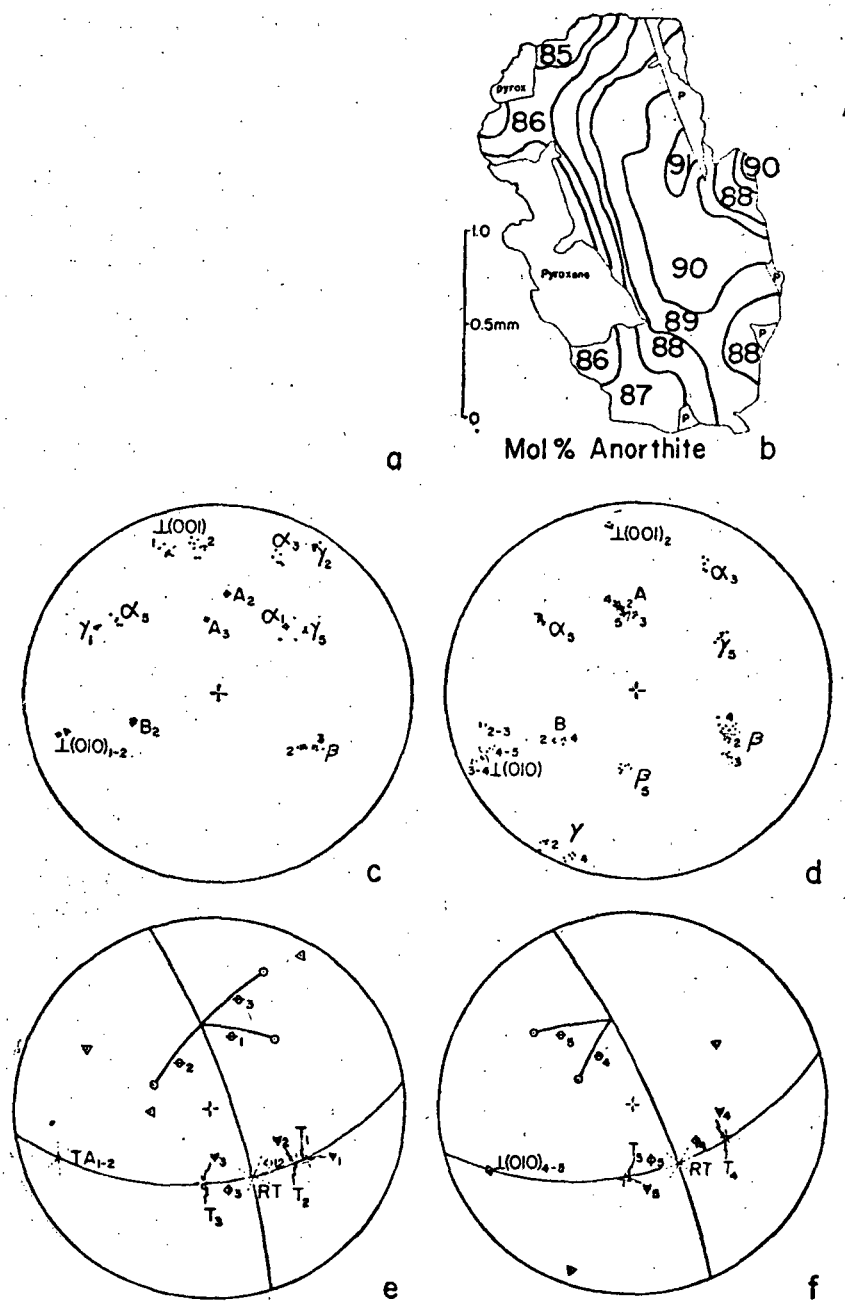

Fig. 1. (a) Photomicrograph of the twin individuals in specimen 12032,44 which have been used in this analysis. Locations of optical and X-ray measurements are indicated (Zeiss Ultraphot III). (b) Map of the crystals, giving chemical composition (An content in mole %). (c–f) Stereograms showing the orientation of the optical indicatrix and the construction of the Euler angles in area A (c, e) and B (d, f). Same orientation as Fig. 1a, upper hemisphere. (c, d) Raw U-stage measurements, A, B = optic axes. (e, f) Construction of Euler angles. ⊙ = α, $\frac{1}{2}$ = β, △ = γ, RT = Roc Tourné twin axis ⊥ [001] in (010).

Table 1. Chemical analyses for lunar bytownite 12032,44 (determined with an ARL microprobe).

	Average of 77 spots over entire specimen	Area A	Area B	Single Crystal	Stoichiometric An_{89} (for comparison)
			weight %		
SiO_2	46.8	46.6	46.3	46.5	46.0
Al_2O_3	33.2	33.5	33.4	33.5	34.8
CaO	17.7	17.9	17.9	17.7	17.9
K_2O	0.01	0.01	0.01	0.01	
Na_2O	1.44	1.32	1.32	1.37	1.30
SrO	0.03	0.03	0.03	0.03	
FeO	0.34	0.33	0.31	0.42	
TOTAL*	99.5	99.7	99.3	99.5	100.0
			Mole %		
An	88.8_8	89.7_0	89.7_6	89.1_3	89.0
Or	0.02	0.03	0.03	0.03	0.0
Ab	11.1_0	10.2_7	10.2_1	10.8_4	11.0

* Low totals due to small errors in the determinations of Al and Si.

Independent raw measurements are shown in Figs. 1c and d. There is some scatter in the data which we attribute partly to difficulties in measuring these relatively small crystals, and also to the limits of resolution of the U-stage. A numerical average of the measurements has been used in the subsequent derivation of the Euler angles (BURRI, 1956) which are used to characterize the orientation of the optical indicatrix. This average appears to be reliable: optical directions were mutually perpendicular within ± 1 deg, the error triangle in the construction of the twin axis was less than 2 deg. Constructed and calculated composition planes agree within 2 deg. The cleavage is poorly developed and has not been used in the analysis. Euler I angles were constructed in group A from optical directions of a complex Albite (1–2)-Roc Tourné (1–3) twin group, constructed and measured poles to (010) (Fig. 1f). The relationship between crystals 3 and 4 is an irrational intergrowth without a twin axis, although the composition plane is a well-developed face approximately parallel to (010).

Euler I angles determined on five crystals are listed on Table 2. The measurements on 2A are least reliable as the thin lamellae overlap partly during tilting and these measurements have been omitted in the calculation of an average. From the averaged Euler I angles and from $2V\gamma = 99\frac{1}{2}$ deg, additional positional angles have been calculated:

Euler II: R = 118.0 deg, I = 91.5 deg, $L\alpha$ = 53.5 deg, L_A = 13.3 deg, L_B = 93.8 deg
Euler III: D = 29.1 deg, N = 53.5 deg, $A\alpha$ = 91.8 deg
Goldschmidt ([001] normal):

ϕ	206.0 deg	298.0 deg	29.1 deg	207.7 deg	49.5 deg
	α	β	γ	A	B
ρ	36.5 deg	88.5 deg	53.5 deg	76.7 deg	4.1 deg

⊢ - Carlsbad (2-3) twin group; constructed and measured poles to (010) were averaged (Fig. 1e). In group B the Euler I angles were derived from a Roc Tourné twin (4-5) and the measured composition plane (010) (Fig. 1f)

In Fig. 2, $\hat{\phi}$ and $\hat{\psi}$ of the lunar bytownite (An 89%) are compared with the curves of BURRI *et al.* (1967) and with the volcanic, An 85% bytownite from Cape Parry (WENK *et al.*, 1968). There is a significant difference in the orientation of the optical indicatrix which suggests that the lunar bytownite may have formed under plutonic rather than under volcanic conditions. The values are intermediate between bytownites from mafic intrusives such as the Bushfeld complex (An 87.5, BURRI *et al.*, 1967) and Åkero in Sweden (An 90.9, NIKITIN, 1933). These data for a plagioclase from 12032,44 are different from the observations of BANCROFT *et al.* (1971) for plagioclase from basaltic rocks 12051, 12052. They describe volcanic optics but no data are presented which would permit a quantitative comparison. Bytownites and anorthites from meteorites were described as having plutonic optical properties (ULBRICH, 1971).

Table 2. Euler angles for lunar plagioclase from rock 12032,44.

		ϕ	θ	ψ	$2V_\gamma$
Group A	1	26°	37°	−2°	
	2	22°	38½°	−1°	98
	3	26°	36°	−3°	98
	5				100
Group B	4	26°	36°	−2°	101
	5	26°	36½°	−3°	97
	2				101
Average		26°	36½°	−2½°	99½

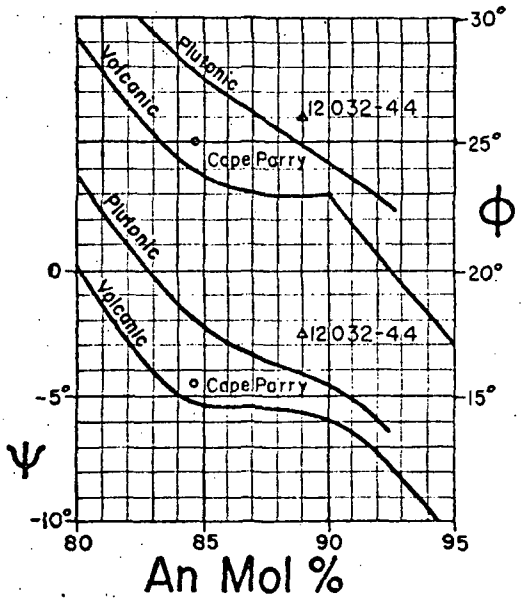

Fig. 2. Diagram of Euler angles ψ and ϕ as a function of the An-content (after BURRI *et al.*, 1968). Lunar bytownite from 12032,44 and volcanic bytownite from Cape Parry (WENK *et al.*, 1969) are indicated.

Refractive indices were measured in fragment R on a spindle stage with oil immersion and Na-light. The small size of the specimen (only 0.02 mm thick) limited us to determinations of α' and γ' in (010).

$$\alpha': 1.576 \pm 0.001 \qquad \gamma': 1.583 \pm 0.001$$

Structure

X-ray single-crystal measurements have been done to determine lattice constants and presence or absence of reflections which are indicative of the structural state. Other investigators describe diffuse to sharp b and diffuse to very diffuse c reflections using X-ray and electron diffraction (Appleman *et al.*, 1971; Bancroft *et al.*, 1971; Christie *et al.*, 1971). An 850 hour precession *a* exposure (Fig. 3a) shows that this bytownite (fragment X, in Fig. 1a) has a body-centered anorthite structure with sharp b reflections. c-reflections were not observed even with long exposure times. c-reflections become diffuse with disorder and increasing albite content. Comparison of the lunar plagioclase with one of identical composition, an An 89 bytownite from a gabbro of the basal zone of the Stillwater complex, removes this ambiguity. The Stillwater bytownite 0kl photograph (Fig. 3b) shows sharp b and moderate but diffuse c-reflections. The apparent absence or extreme weakness of c-reflections in the lunar bytownite (Fig. 3a) indicates that it is more disordered than the terrestrial one. This differs from plagioclase from some lunar "basalts" which have a "low structural state" (Appleman *et al.*, 1971, p. 8).

Lattice constants were determined from sets of precession photographs on the fragment X (Fig. 1a): $a_0 = 8.16$ Å $\pm$ 0.01; $b_0 = 12.89$ Å $\pm$ 0.01; $c_0 = 14.18$ Å $\pm$ 0.01; $\alpha = 93.53° \pm 0.1$; $\beta = 115.8° \pm 0.1$; $\gamma = 90.8° \pm 0.1$; V = 1338.0 Å^3; $\gamma^* = 87.4° \pm 0.1$. They compare well with data given by Appleman *et al.* (1971) but are inconclusive with respect to the structural state.

ILLUSTRATION

Fig. 3. Precession 0kl-photographs of bytownites. b* is horizontal. Mo radiation, Zr filter, b ($h + k$ odd, l odd), and c ($h + k$ even, l odd) reflections are indicated. (a) Lunar bytownite An 89, X (Fig. 1a), from 12032,44. 850-hour exposure. (Includes faint albite twin.) Note absence of c-reflections. (b) Bytownite An 89, from a gabbro of the Stillwater complex, 50-hour exposure. Note diffuse but moderately intensive c-reflections.

In the bytownite from 12032,44 optical measurements indicate plutonic properties whereas X-ray data indicate a partially disordered structure. It appears to be another case where "disordered" structure does not correpond to volcanic optics (cf. WENK, 1969). The relationship between optical and structural parameters is the subject of a current experimental investigation. It seems that there is no simple direct correlation between the two, although in most cases "volcanic optics" is found in feldspar with a disordered structure.

Acknowledgments—The authors are indebted to Professor P. B. Price for the specimen, J. Hampel for photographic work, and R. Barker kindly supplied a specimen of Stillwater bytownite. The work has been supported by NASA grants NGR 05-002-414 and NGR 05-003-410.

REFERENCES

APPLEMAN D. E., NISSEN H. U., STEWART D. B., CLARK J. R., DOWTY E., and HUEBNER J. S. (1971) Crystallographic studies of Apollo 11 and Apollo 12 plagioclase, tridymite, and cristobalite. Second Lunar Science Conference (unpublished proceedings).

BANCROFT G. M., BROWN M. G., GAY P., MUIR I. D., and WILLIAMS P. G. L. (1971) Mineralogical and petrographic investigation of some Apollo 12 samples. Second Lunar Science Conference (unpublished proceedings).

BURRI C. (1956) Charakterisierung der Plagioklasoptik durch drei Winkel und Neuentwurf des Stereogramms der optischen Orientierung für Konstante Anorthit-Intervalle. *Schweiz. mineral. petrog. Mitt.* **36**, 539–592.

BURRI C., PARKER R. L., and WENK E. (1967) *Die optische Orientierung der Plagioklase*. Birkhäuser, Basel.

CHRISTIE J. M., FISHER R. M., GRIGGS D. T., HEUER A. H., LALLY J. S., and RADCLIFFE S. V. (1971) Comparative electron petrography of Apollo 11, Apollo 12, and terrestrial rocks. Second Lunar Science Conference (unpublished proceedings).

NIKITIN W. W. (1933) Korrekturen and Vervollständigungen der Diagramme zur Bestimmung der Feldspate nach Fedorows Methode. *Mineral. petrog. Mitt. Tscherm.* [N. F.] **44**, 117–167.

ULBRICH M. (1971) Systematics of eucrites and howardite meteorites and a petrographic study of representative individual eucrites. M.A. thesis, University of California, Berkeley.

VIRGO D., HAFNER S. S., and WARBURTON D. (1971) Cation distribution studies in clinopyroxenes, olivines, and feldspars using Mössbauer spectroscopy of ^{57}Fe. Second Lunar Science Conference (unpublished proceedings).

WENK E., WENK H.-R., and SCHWANDER H. (1968) Bytownite from Cape Parry, East Greenland. *Amer. Mineral.* **53**, 1759–1764.

WENK H.-R. (1969) Annealing of oligoclase at high pressure. *Amer. Mineral.* **54**, 95–100.

WOOD J. A., MARVIN V., REID J. B., TAYLOR G. J., BOWER J. F., POWELL B. N., and DICKEY J. S., JR. (1971) Relative proportions of rock types, and nature of the light-colored lithic fragments in Apollo 12 soil samples. Second Lunar Science Conference (unpublished proceedings).

STRUCTURE REFINEMENTS OF FOUR OLIVINES

H.-R. Wenk and K. N. Raymond

(Department of Geology and Geophysics, and Department of Chemistry, University of California at Berkeley)

Abstract

Much work has been invested in recent years in the study of the olivine structure with the main emphasis to determine Mg/Fe order. Such order has been suggested from X-ray data (Finger, 1970) and proven with Mössbauer spectra (Bush et al., 1970). We present here results of X-ray structure refinements for two metamorphic forsterites (Fa 0 and Fa 10) and two lunar Fa 30 olivines. Extinction coefficient, atomic positions, anisotropic thermal parameters, site occupancies and formal charges were refined by least squares methods, imposing proper constraints of chemical composition and electrostatic neutrality on derivatives. The results show good agreement for positional parameters with previous investigations. No order has been found in forsterite, but the lunar samples show significant (20 standard deviations) order of Fe on the M(1) site (52%). Many more refinements are necessary before Fe/Mg order in olivines can be used to interpret the geological history of a rock, but it appears that the (Fe(1)/Fe(2)) ratio is fixed very early during crystallization of the mineral. Formal charges have been determined: Fe, Mg = +0.3, Si = +0.2; O = -0.2. The extinction coefficient, a sensitive measure of structural defects, varies by an order of magnitude. It is especially low for a specimen from lunar dust which is expected to have defects from cosmic radiation and shock deformation. R factors range between 2 and 3%.

Introduction

Bragg and Bowen (1926) determined the basic structure of olivine and found hexagonal close packing of oxygen with Mg, Fe occupying half of the distorted octahedral (M(1) and M(2)) and Si half of the tetrahedral sites (Figure 1). There have been refinements done on olivines of different compositions with emphasis on the determination of structural variations in this Mg-Fe solid solution series. But until recently no deviations from ideal substitution could be determined in these refinements (Belov et al., 1951; Born, 1964; Hanke and Zemann, 1963; Hanke, 1963; Birle et al., 1968). Eliseev (1958) reported deviations of the lattice parameters from Vegard's rule in the fayalite-forsterite solid solution series, which was probably based on inaccurate chemical data. Ghose (1962) predicted that Fe would be preferentially ordered on the larger M(2) site. These suggestions and the fact that in isostructural compounds like monticellite, $CaMgSiO_4$ (Onken, 1965) and glaucochroite, $CaMnSiO_4$ (Caron et al., 1965) the cations are ordered encouraged other investigators not to give up the search for order in olivines and it was with spectroscopic methods that partial order has first been determined in intermediate olivines (Burns, 1969; Bush et al., 1970). The latest development in X-ray single crystal diffractometers greatly enhance the resolution of a standard crystal structure refinement and it becomes possible to determine electron densities in fractions of an electron. The latest refinements of Finger (1969/70) suggest order of Fe on the M(1) site of a 50% forsterite within four standard deviations. With this background in mind, the present investigation has been started. The aim was to obtain more accurate data on the geologically more important magnesium-rich olivines.

Experimental procedure

Small crystals (0.1-0.2 mm) of isometric shape were selected from various rock specimens; two are metamorphic forsterites and two are intermediate (Fa 30) olivines from lunar basalt. Specifications are given in Table 1. The crystals were first checked on a precession camera for space group, domain structure and asterism. For all of them the space group Pbnm was determined. No extra reflections have been observed (Eliseev, 1958). Then the crystals were oriented on a computer-controlled Picker diffractometer. From the positions of twelve reflections the lattice constants and the orientation angles were refined by least squares (Table 2). They agree closely with the determinative curves of Yoder and Sahama (1957); Jambor and Smith (1964) or Jahanbagloo (1969). Data were collected by the θ-2θ scan technique to Bragg angles of 100° using monochromatic MoK_α radiation. Highly oriented graphite was used as monochromator crystal. The 2θ scan width was 1.4° + $\Delta 2\theta$ where $\Delta 2\theta$ is the distance between the calculated maxima for the K_α, and K_{α_2} peaks. The scanning rate was 1 degree per minute with 10 second stationary background counts on either side of the scan. Standard deviations of individual reflections were determined from counting statistics of integrated count and background. An additional error of 3% of the net intensity was added to the standard deviation to avoid overweighting of intense reflections. The raw intensities were corrected for Lorentz-polarization. An absorption correction was not found to be necessary. The intensities from equivalent reflections were then averaged and systematic extinctions rejected. Further information about the specimens and the data collection and data processing is given in Table 4. After the data collection the crystals were analyzed chemically with the microprobe. During this procedure the Apollo 11 crystal was lost. The chemical analysis was done on another olivine crystal from the same rock.

Least squares refinement

The refinement of the structure was done with a modified version of the Busing-Levy least squares program (Busing et al., 1962). Atomic scattering factors were interpolated from the table of Cromer and Waber (1968). Real and imaginary anomalous scattering factors were used for Fe (Cromer, 1965). Several assumptions for the structure model were made: a) there are no vacancies, b) traces of Mn and Ni are closely related to iron and the atomic scattering factors were adjusted accordingly, c) all Ca is on the M(2) site in analogy to montiallite, d) the overall electrical charge is zero, e) all oxygen has equal charge, f) the degree of ionization of Fe and Mg is equal. All refined parameters are relatively insensitive to each of these assumptions. Errors in the chemical analysis are mainly expressed in the refined electrical charge. 44 positional, thermal and scale parameters were refined using imposing proper constraints on the derivatives: a) atomic coordinates of M(2), Si, O(1), O(2), and O(3), b) anisotropic temperature factors for all atoms, c) occupancy factor and ionic charge for Fe(1), Fe(2) and Si, d) an overall extinction factor. After a few cycles the refinement converged with R-factors of 2-3%.

The least squares refinement of site occupancies has to take into account constraints imposed by the chemical composition and overall electrostatic neutrality.* Raymond (1971) derived the formal solution of the general problem. Crystal has n atoms and each atom has a multiplicity factor a_i. We cannot refine all of these multiplicity factors because of constraints. For instance we have to impose electrical neutrality of the crystal and the chemical formula in a solid solution. If there are n atoms and n linear equations of constraint, then there are only k = n - m independent variables

*If many independent and correlated constraints are acting then the effect on the derivatives is no longer trivial. A detailed specification of variables and constraints for each crystal is necessary so that the reader can evaluate the resolution which is forced to the limits of small fractions of an electron.

V_k. We form a square matrix Q by combining independent variables with the constraints. In the following discussion, variables and constraints are specified for each crystal. For the Yosemite forsterite with very little Fe the refinement has been done on the basis of the formula $(Mg, Fe)SiO_4$ with 6 atoms (M(1), M(2), Si, O(1), O(2), O(3)). Occupancies of M(1), M(2) and M(3) were refined, thus the matrix becomes

$$Q = \begin{array}{c} \begin{matrix} a_{M(1)} & a_{M(2)} & a_{Si} & a_{O(1)} & a_{O(2)} & a_{O(3)} \end{matrix} \\ \begin{pmatrix} 1 & 0 & 0 & 0 & 0 & 0 \\ 0 & 1 & 0 & 0 & 0 & 0 \\ 0 & 0 & 1 & 0 & 0 & 0 \\ 12.203 & 12.203 & 14 & 8 & 8 & 8 \\ 0 & 0 & 0 & 1 & -1 & 0 \\ 0 & 0 & 0 & 2 & 0 & -1 \end{pmatrix} \end{array} \begin{matrix} V_1 \\ V_2 \\ V_3 \\ C_1 = 35.203 \\ C_2 = 0 \\ C_3 = 0 \end{matrix}$$

Constraint c_1 ensures that electrostatic neutrality is maintained. Constraints c_2 and c_3 impose equal occupancy on the oxygen sites. From the refined occupancies the formal electrical charge q can be calculated

$$q = \frac{Z(a_i^0 - a_i)}{a_i}$$

where a_i^0 is the occupancy in the chemical formula and a_i is the refined occupancy. Z is the atomic number of the element.

In the case of the Bergell olivine Sci 59 the relation is more complicated. There is now sufficient Fe to separate the M-sites into an Fe and an Mg contribution. Traces of other transition elements (e.g., Ni, Mn) are combined with the chemically similar Fe. The formula is $Fe_{0.107}Mg_{0.893}SiO_4$

with eight atoms (Fe(1), Fe(2), Si, Mg(1), Mg(2), O(1), O(2), O(4)). Occupancies of Fe(1), Fe(2) and Si were refined and two additional constraints were introduced. C_1 imposes equal occupancy of M(1) and M(2), and C_2 introduces the Fe/Mg ratio obtained from the chemical analysis. Formal charges q were taken into account. The equations are no longer strictly linear and were reset for q after every cycle in the refinement.

$$Q = \begin{array}{c} \begin{matrix} a_{Fe(1)} & a_{Fe(2)} & a_{Si} & a_{Mg(1)} & a_{Mg(2)} & a_{O(1)} & a_{O(2)} & a_{O(3)} \end{matrix} \\ \begin{pmatrix} 1 & 0 & 0 & 0 & 0 & 0 & 0 & 0 \\ 0 & 1 & 0 & 0 & 0 & 0 & 0 & 0 \\ 0 & 0 & 1 & 0 & 0 & 0 & 0 & 0 \\ b_1 & -b_1 & 0 & b_2 & -b_2 & 0 & 0 & 0 \\ b_1 & b_1 & 0 & -b_2 \cdot \frac{Fe}{Mg} & -b_2 \cdot \frac{Fe}{Mg} & 0 & 0 & 0 \\ 26.134 & 26.134 & 14 & 12.0 & 12.0 & 8 & 8 & 8 \\ 0 & 0 & 0 & 0 & 0 & -1 & 1 & 0 \\ 0 & 0 & 0 & 0 & 0 & -2 & 0 & 1 \end{pmatrix} \end{array} \begin{array}{l} V_1 \\ V_2 \\ V_3 \\ C_1 = 0 \\ C_2 = 0 \\ C_3 = 36.500 \\ C_4 = 0 \\ C_5 = 0 \end{array}$$

where $b_1 = \frac{26.134 + q}{26.134}$, $b_2 = \frac{12.0 + q}{12.0}$ and Fe/Mg = 0.1198.

The lunar samples Apollo 11 and Apollo 12 contain enough Ca to treat it as a separate atom. In the isostructural Monticellite ($CaMgSiO_4$) Ca is ordered on the M(2) site (Onken, 1965) and it was placed there in analogy. The formula becomes for Apollo 11 $Fe_{0.300}Mg_{0.695}Ca_{0.005}SiO_4$ and for Apollo 12 $Fe_{0.323}Mg_{0.672}Ca_{0.004}SiO_4$ with nine atoms (Fe(1), Fe(2), Si, Mg(1), Mg(2), Ca(2), Si, O(1), O(2), O(3)) used in the refinement. The same independent variables were used as before.

$$
Q = \begin{array}{c}
\begin{array}{ccccccccc}
a_{Fe(1)} & a_{Fe(2)} & a_{Si} & a_{Mg(1)} & a_{Mg(2)} & a_{Ca(2)} & a_{O(1)} & a_{O(2)} & a_{O(3)}
\end{array} \\
\left(\begin{array}{ccccccccc}
1 & 0 & 0 & 0 & 0 & 0 & 0 & 0 & 0 \\
0 & 1 & 0 & 0 & 0 & 0 & 0 & 0 & 0 \\
0 & 0 & 1 & 0 & 0 & 0 & 0 & 0 & 0 \\
-b_1 & -b_1 & 0 & b_2 & -b_2 & -1 & 0 & 0 & 0 \\
b_1 & b_1 & 0 & -b_2 \cdot \frac{Fe}{Mg} & -b_2 \cdot \frac{Fe}{Mg} & 0 & 0 & 0 & 0 \\
0 & 0 & 0 & 0 & 0 & 1 & 0 & 0 & 0 \\
\begin{array}{l}26.0\ (11) \\ 26.015\ (12)\end{array} & \begin{array}{l}26.0 \\ 26.015\end{array} & 14. & 12. & 12. & 20 & 8. & 8. & 8. \\
0 & 0 & 0 & 0 & 0 & 0 & \bar{1} & 1 & 0 \\
0 & 0 & 0 & 0 & 0 & 0 & \bar{2} & 0 & 1
\end{array}\right)
\end{array}
\begin{array}{l}
V_1 \\ V_2 \\ V_3 \\ C_1 = 0 \\ C_2 = 0 \\ C_3 = 0.005 \\ C_4 = \begin{array}{l}39.24 \\ 39.56\end{array} \\ C_5 = 0 \\ C_6 = 0
\end{array}
$$

with $b_1 = \frac{26 + q}{26}$, $b_2 = \frac{12 + q}{12}$ and Fe/Mg = .4317 for Apollo 11 and

$b_1 = \frac{26.015 + q}{26.015}$, $b_2 = \frac{12 + q}{12}$ and Fe/Mg = .4927 for Apollo 12.

Table 2. Physical Properties of Olivines

	Yosemite 103-481	Bergell Alps Sci 59	Oceanus Procellarum Apollo 12 12070-12.4	Mare Tranquillitatis Apollo 11 10085
lattice constants (Pbnm setting)				
a_0	4.7533 (5) Å[1]	4.7623 (4) Å	4.7748 (5) Å	4.7768 (6) Å
b_0	10.1972 (7) Å	10.2284 (11) Å	10.2798 (16) Å	10.2943 (16) Å
c_0	5.9821 (3) Å	5.9942 (6) Å	6.0087 (9) Å	6.0174 (9) Å

[1] In this and the following rables standard deviations in the least significant digits are given in parentheses.

Table 3. Chemical Composition of Olivines (microprobe analyses).

	Yosemite 103-481	Bergell Alps Sci 59	Oceanus Procellarum Apollo 12 12070-12.4	Mare Tranquillitatis Apollo 11 10085 (1)
weight percent				
SiO_2	42.21%	~37.79%	37.10	36.88
FeO	1.21%	9.25%	27.53	26.37
TiO_2	--			
MnO	0.29%	0	0	0
NiO	traces	0.74%	0.37	0
MgO	56.03%	49.30%	34.17	35.95
CaO	0.06%	0.02%	0.35	0.36
Na_2O	--			
Total	99.80%	97.1%	99.52	99.56
formula used in refinement				
Fe	0.012	0.099	0.319	0.300 (2)
Mn	0.003	--	--	--
Ni	0	0.008	0.004	0
Mg	0.985	0.893	0.672	0.695
Ca	< 0.001	0	0.005	0.005
Si	0.5	0.5	0.5	0.5
O	2	2	2	2
refined formula from X-ray data				
Fe				0.358 (5)
Mg				0.637
Ca				0.005

(1) chemical analysis done on different crystal from the same rock.
(2) later replaced by formula below.

Table 4. X-ray Data Collection

	Yosemite 103-481	Bergell Alps Sci 59	Oceanus Procellarum Apollo 12 12070-12.4	Mare Tranquillitatis Apollo 11 10085
crystal size	0.15 x 0.15 x 0.15 mm	0.15 x 0.10 x 0.10 mm	0.2 x 0.15 x 0.1 mm	0.3 x 0.2 x 0.2 mm
linear absorption coefficient μ	11. cm^{-1}	19. cm^{-1}	40. cm^{-1}	45. cm^{-1}
total number of observations	1427	3644	2349	3161
number of independent observations	1125	1797	1321	2029
number of independent reflections used in refinement ($\|F\|^2>3\sigma$)	783	851	882	1459
R-factor (all data)	.023	.022	.022	.022
Weighted R (all data)	.032	.026	.029	.032

Table 5. Atomic Parameters of Olivine

	Yosemite 103-481	Bergell Alps Sci 59	Oceanus Procellarum Apollo 12 12070-12.4	Mare Tranquillitatis Apollo 11 10085
M(1)				
x=y=z=0				
M(2)				
x	.99119 (10)	.98968 (8)	.98765 (7)	.98724 (5)
y	.27744 (4)	.27772 (4)	.27821 (3)	.27842 (2)
z = 1/4				
Si				
x	.42625 (7)	.42681 (7)	.42752 (7)	.42786 (5)
y	.09409 (4)	.09443 (4)	.09521 (4)	.09535 (3)
z = 1/4				
O(1)				
x	.76557 (20)	.76589 (18)	.76603 (19)	.76645 (13)
y	.09144 (9)	.09148 (9)	.09185 (9)	.09211 (7)
z = 1/4				
O(2)				
x	.22163 (20)	.22066 (19)	.21720 (20)	.21690 (14)
y	.44721 (8)	.44767 (8)	.44882 (8)	.44930 (6)
z = 1/4				
O(3)				
x	.27723 (12)	.27838 (13)	.28034 (13)	.28122 (9)
y	.16311 (6)	.16333 (6)	.16381 (6)	.16406 (5)
z	.03315 (11)	.03329 (10)	.03431 (10)	.03422 (8)

Table 6. Site Occupancies and Apparent Charges of Olivines

	Yosemite 103-481	Bergell Alps Sci 59	Oceanus Procellarum Apollo 12 12070-12.4	Mare Tranquillitatis Apollo 11 10085
occupancies				
M(1)				
Fe	.4976 (8)	.0526 (6)	1.672 (6)	.1871 (7)
Mg		.4474	.3328	.3129
M(2)				
Fe		.0541 (6)	.1558 (4)	.1709 (7)
Mg	.5023 (8)	.4459	.3392	.3241
Ca	--	--	.005	.005
K_D	(.66 (20))	.969 (24)	1.096 (10)	1.134 (11)
charges per atom				
M(1)=M(2)	+.33 (3)	+.22 (3)	.34 (4)	.13 (5)
Si	+.27 (3)	+.20 (8)	+.03 (3)	.14 (3)
O(1)=O(2)=O(3)	-.23	-.15	-.18	-.10
extinction coefficient	$.90(4).10^{-6}$	$2.94(11).10^{-6}$	$0.15(4).10^{-6}$	$0.27(2).10^{-6}$

Table 7. Thermal parameters of olivines ($\beta \times 10^5$)
(temperature factors are of the form $\exp[-(\beta_{11}h^2 + \beta_{22}k^2 + \beta_{33}\ell^2 + 2\beta_{12}hk + 2\beta_{13}h\ell + 2\beta_{33}k\ell)]$

	Yosemite 103-481	Bergell Alps Sci 59	Oceanus Procellarum Apollo 12 12070-12.4	Mare Tranquillitatis Apollo 11 10085
M(1)				
β_{11}	333 (15)	287 (12)	498 (10)	417 (6)
β_{22}	140 (3)	110 (3)	162 (3)	147 (2)
β_{33}	316 (10)	214 (8)	204 (7)	347 (4)
β_{12}	-9 (5)	0 (5)	-4 (3)	-5 (2)
β_{13}	-43 (9)	-40 (7)	-36 (5)	-45 (3)
β_{23}	-34 (5)	-36 (4)	-41 (3)	-41 (2)
M(2)				
β_{11}	418 (17)	470 (14)	692 (13)	585 (7)
β_{22}	99 (4)	69 (3)	106 (2)	94 (1)
β_{33}	375 (11)	269 (8)	240 (7)	365 (4)
β_{12}	9 (6)	2 (5)	14 (4)	2 (2)
$\beta_{13}=\beta_{23}=0$				
Si				
β_{11}	178 (12)	133 (11)	340 (11)	257 (7)
β_{22}	88 (3)	56 (2)	99 (2)	89 (2)
β_{33}	284 (8)	179 (6)	172 (7)	301 (5)
β_{12}	2 (4)	4 (4)	9 (4)	13 (2)
$\beta_{13}=\beta_{23}=0$				
O(1)				
β_{11}	389 (26)	238 (24)	493 (26)	369 (14)
β_{22}	164 (7)	145 (6)	179 (6)	172 (3)
β_{33}	436 (18)	329 (16)	285 (15)	431 (11)
β_{12}	5 (10)	11 (11)	7 (10)	15 (6)
$\beta_{13}=\beta_{23}=0$				
O(2)				
β_{11}	530 (27)	501 (27)	699 (27)	619 (17)
β_{22}	124 (6)	84 (6)	114 (5)	103 (3)
β_{33}	466 (18)	326 (16)	358 (15)	463 (11)

β_{11}	333 (15)	287 (12)	498 (10)	417 (6)
β_{22}	140 (3)	110 (3)	162 (3)	147 (2)
β_{33}	316 (10)	214 (8)	204 (7)	347 (4)
β_{12}	-9 (5)	0 (5)	-4 (3)	-5 (2)
β_{13}	-43 (9)	-40 (7)	-36 (5)	-45 (3)
β_{23}	-34 (5)	-36 (4)	-41 (3)	-41 (2)
M(2)				
β_{11}	418 (17)	470 (14)	692 (13)	585 (7)
β_{22}	99 (4)	69 (3)	106 (2)	94 (1)
β_{33}	375 (11)	269 (8)	240 (7)	365 (4)
β_{12}	9 (6)	2 (5)	14 (4)	2 (2)
$\beta_{13}=\beta_{23}=0$				
Si				
β_{11}	178 (12)	133 (11)	340 (11)	257 (7)
β_{22}	88 (3)	56 (2)	99 (2)	89 (2)
β_{33}	284 (8)	179 (6)	172 (7)	301 (5)
β_{12}	2 (4)	4 (4)	9 (4)	13 (2)
$\beta_{13}=\beta_{23}=0$				
O(1)				
β_{11}	389 (26)	238 (24)	493 (26)	369 (14)
β_{22}	164 (7)	145 (6)	179 (6)	172 (3)
β_{33}	436 (18)	329 (16)	285 (15)	431 (11)
β_{12}	5 (10)	11 (11)	7 (10)	15 (6)
$\beta_{13}=\beta_{23}=0$				
O(2)				
β_{11}	530 (27)	501 (27)	699 (27)	619 (17)
β_{22}	124 (6)	84 (6)	114 (5)	103 (3)
β_{33}	466 (18)	326 (16)	358 (15)	463 (11)
β_{12}	2 (11)	10 (10)	4 (11)	-12 (6)
$\beta_{13}=\beta_{23}=0$				
O(3)				
β_{11}	514 (19)	445 (17)	634 (19)	576 (12)
β_{22}	172 (5)	127 (4)	182 (4)	161 (3)
β_{33}	445 (13)	326 (11)	320 (11)	445 (8)
β_{12}	1 (8)	24 (7)	13 (7)	25 (5)
β_{13}	-22 (13)	-15 (12)	-25 (11)	-10 (8)
β_{23}	45 (6)	54 (5)	70 (5)	66 (4)

Table 8. Selected interatomic distances (Å) of olivines.

	Yosemite 103-481	Bergell Alps Sci 59	Oceanus Procellarum Apollo 12 12070-12.4	Mare Tranquillitatis Apollo 11 10085
Si-tetrahedron				
1 Si - O(1)	1.6131(10)	1.6150(9)	1.6167(10)	1.6177(7)
1 O(2)	1.6545(9)	1.6572(9)	1.6559(10)	1.6549(7)
2 O(3)	1.6370(7)	1.6382(7)	1.6343(6)	1.6361(5)
mean	1.6354	1.6372	1.6353	1.6362
1 O(1)-O(2)	2.7434(13)	2.7445(13)	2.7360(14)	2.7371(10)
-O(3)	2.7577(10)	2.7600(6)	2.7577(10)	2.7580(8)
1 O(2)-O(3)[a]	2.5553(10)	2.5599(10)	2.5620(10)	2.5639(8)
1 O(3)-O(3)[a]	2.5945(13)	2.5980(13)	2.5920(12)	2.5968(11)
M(1)-octahedron				
2 M(1)-O(1)	2.0851(6)	2.0891(6)	2.0967(7)	2.0992(5)
2 -O(2)	2.0681(6)	2.0741(6)	2.0873(7)	2.0891(5)
2 -O(3)	2.1313(6)	2.1420(6)	2.1610(7)	2.1678(5)
mean	2.0948	2.1017	2.1150	2.1187
2 O(1)-O(2)[b]	2.847	2.854	2.872	2.873
2 -O(2)	3.0241(2)	3.0314(4)	3.0423(5)	3.0479(5)
2 -O(3)[b]	2.8516(11)	2.8608(10)	2.8735(10)	2.8777(8)
2 -O(3)	3.106	3.118	3.218	3.151
2 O(2)-O(3)[a]	2.5553(10)	2.5599(10)	2.5620(10)	2.5639(8)
-O(3)	3.3330(9)	3.3507(10)	3.3896(11)	3.3990(8)
M(2)-octahedron				
1 M(2)-O(1)	2.1788(10)	2.1829(10)	2.1886(11)	2.1889(8)
1 -O(2)	2.0487(10)	2.0571(9)	2.0682(10)	2.0731(7)
2 -O(3)	2.2114(8)	2.2241(7)	2.2396(7)	2.2459(6)
2 -O(3)	2.0666(7)	2.0639(7)	2.0624(7)	2.0601(5)
mean	2.1306	2.1360	2.1435	2.1456
2 O(1)-O(3)[b]	2.8516(11)	2.8608(10)	2.8735(10)	2.8777(8)
2 -O(3)	3.0226(10)	3.0293(10)	3.0384(10)	3.0382(8)
2 O(2)-O(3)	3.1852(10)	3.1972(10)	3.2179(11)	3.2235(9)
2 -O(3)	2.9320(9)	2.9341(9)	2.9343(10)	2.9357(7)
1 O(3)-O(3)[a]	2.5945(13)	2.5980(13)	2.5920(12)	2.5968(11)
2 -O(3)	3.3876(13)	3.3962(13)	3.4167(13)	3.4206(11)
2 -O(3)	2.9910(8)	2.9955(8)	3.0016(8)	3.0008(7)

a. edges shared between tetrahedron and octahedron

b. edges shared between octahedra

NO. 341-M DIETZGEN GRAPH PAPER
MILLIMETER
EUGENE DIETZGEN CO.
MADE IN U. S. A.

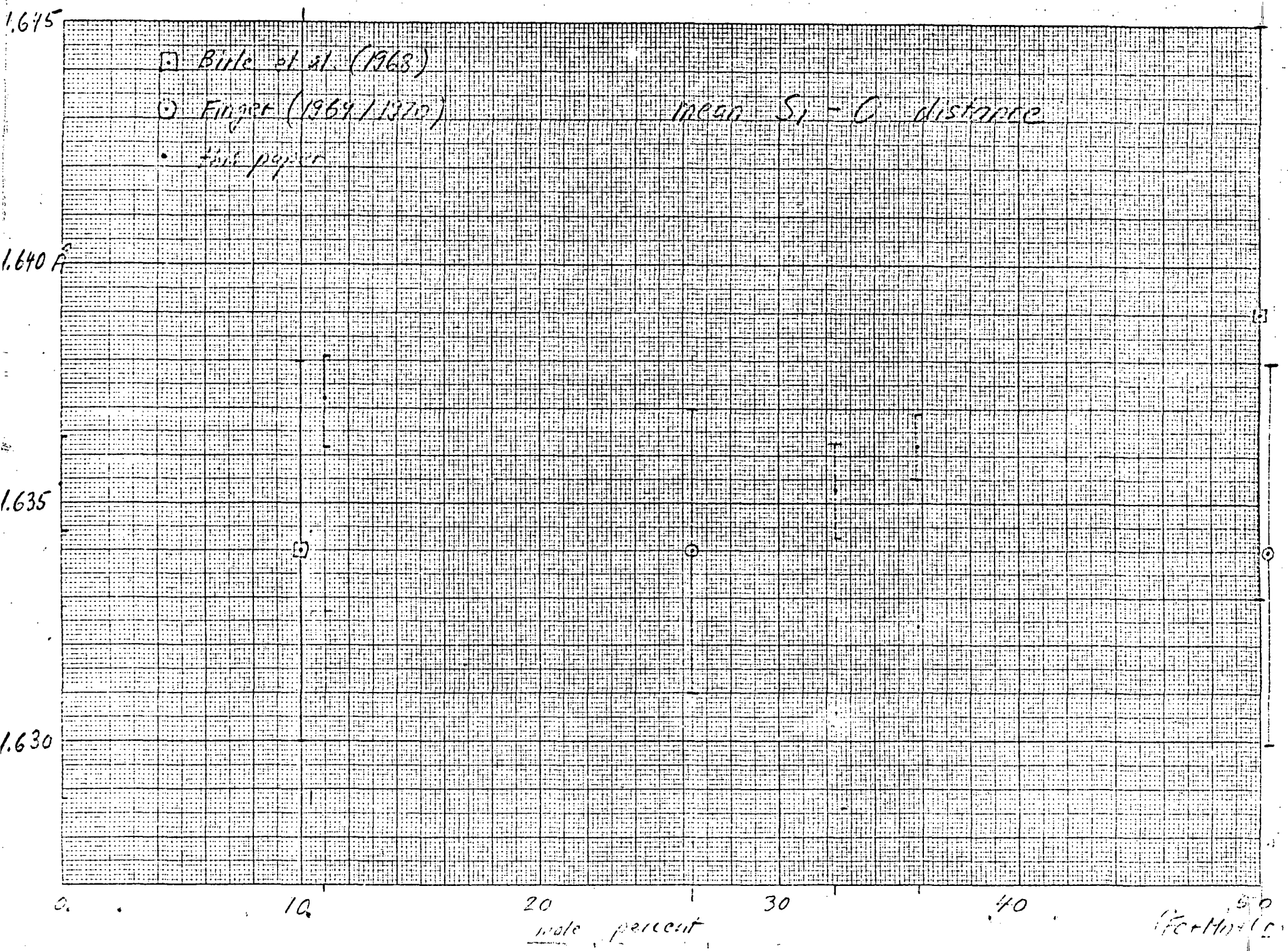

NO. 341-M DIETZGEN GRAPH PAPER
MILLIMETER

EUGENE DIETZGEN CO.
MADE IN U. S. A.

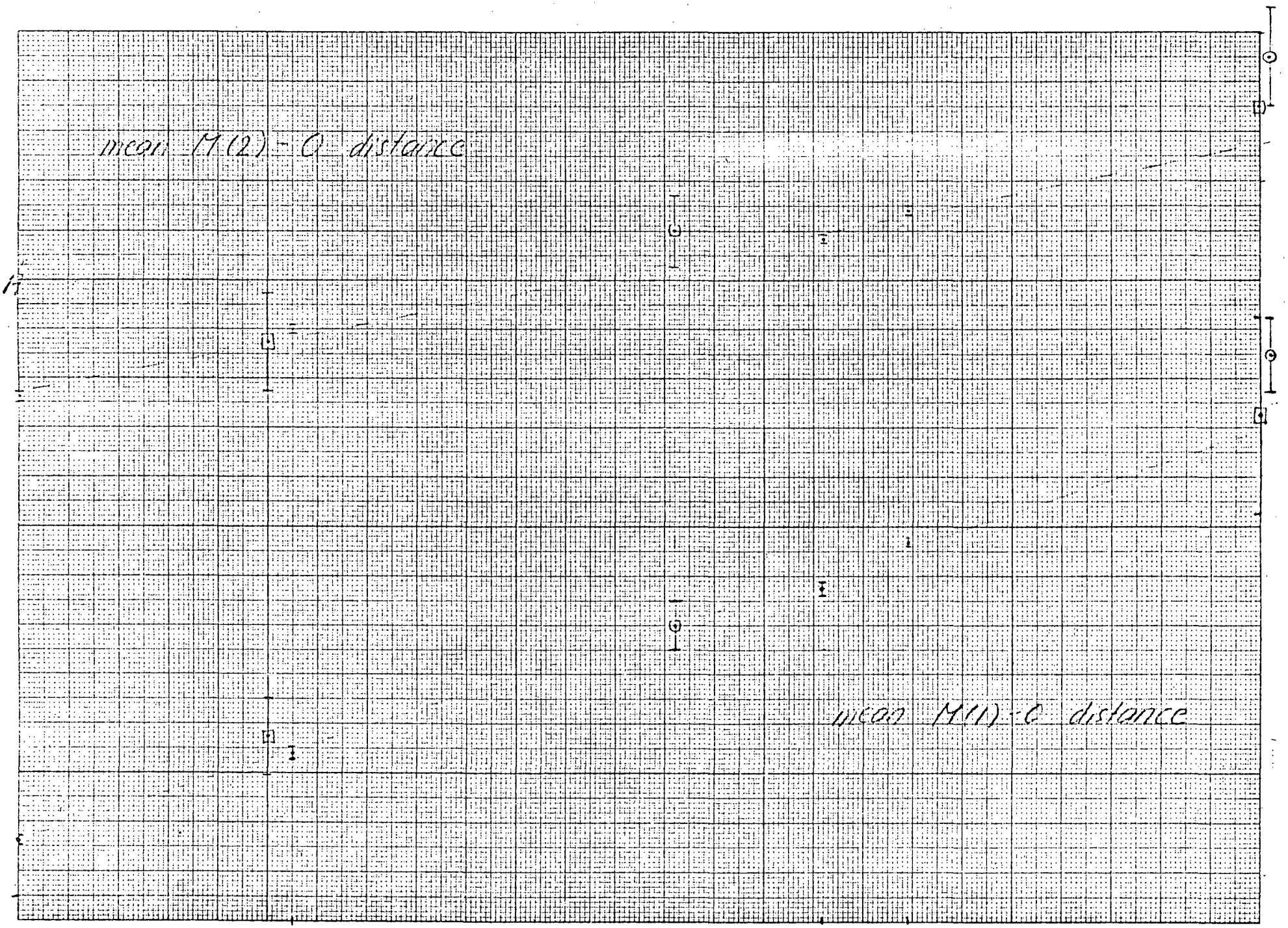

NO. 341-M DIETZGEN GRAPH PAPER
MILLIMETER

EUGENE DIETZGEN CO.
MADE IN U. S. A.

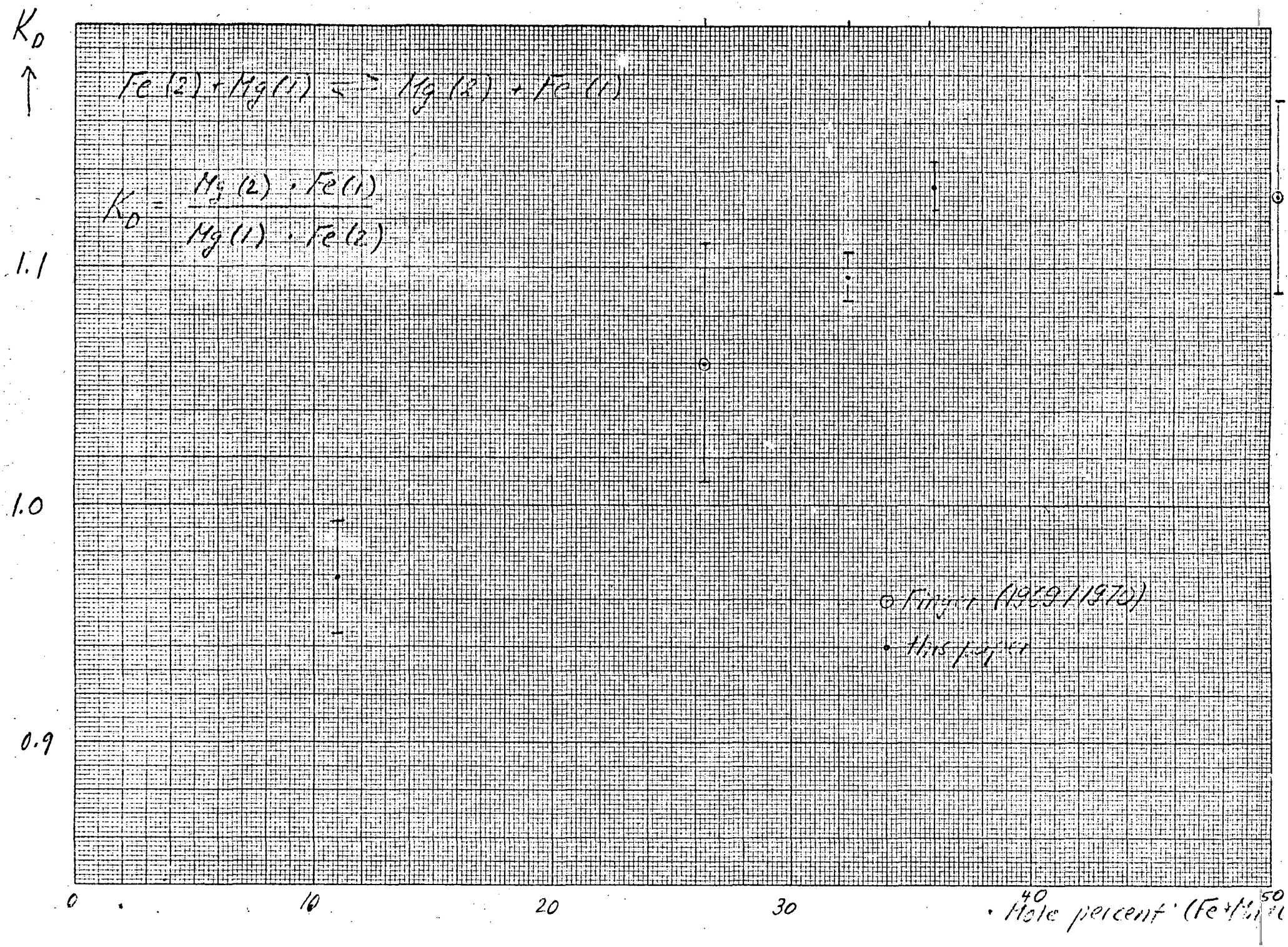

(7)

American Mineralogist
in press

Mounting Methods for Mineral Grains to be Examined by High Resolution Electron Microscopy

D.J. Barber†

Physics Department, University of California, Berkeley
California 94720

ABSTRACT

Small mineral grains (~0.1 - 5μm diameter) are given mechanical and electrical stability by embedding them in an evaporated carbon film. Larger grains (up to ~1 mm diameter) are embedded in a matrix of fine aluminum oxide powder bonded with epoxy resin and thinned by grinding followed by sputter-etching.

This note describes preparation methods which have proved extremely valuable in electron microscope studies of lunar fines in the size range 0.1μm to 5mm diameter. The procedures are applicable to all particulate materials with low solubilities in water and organic media. The examination of mineral grains in transmission has been greatly facilitated by the advent of the sputter-etching method, (Tighe, 1968 and Barber, 1970), and high voltage electron microscopes. However, the advantages of applying high resolution and selected area diffraction methods to minerals (McConnell, 1967) may be lost unless: (a) small grains can be held firmly and prevented from electrical charging in the electron beam; (b) large grains can be supported throughout their thinning by sputter-etching and subsequently made to meet the conditions (a). Ways of achieving these ends will now

† On leave from the University of Essex, Colchester, Essex, England.

be described.

(a) It is common practice to sandwich insulating particles between two evaporated carbon films affixed to support grids. Sometimes this is adequate but it provides less stability with equiaxed particles than with lamellae. Potential problems are avoided by embedding grains of diameter ~0.1 to 5μm within a single carbon film. The fragments are scattered on a clean glass microscope slide which is carbon coated in an evaporator. It is desirable to place the carbon source to one side of the slide and rotate the latter during evaporation so that particles are 'shadowed' from all sides and totally coated. The film, typically 500 to 1000 Å thick, is then stripped from the slide by flotation onto water in the conventional way, so carrying the grains with it. Pieces of film are picked up on 200 mesh grids. Apart from giving particle stability and ease of handling, the method has other advantages. The grains can be chemically treated since the carbon film is permeable but unreactive. If the particles dissolve, the carbon envelopes remain as a record of their original sizes and shapes. Figure 1 shows a heavily etched particle from which approximately 0·2μm has been removed, together with two smaller rounded particles. Because unetched lunar fines usually possess an amorphous skin, caused by solar wind irradiation (Dran et al (1970), Barber et al (1971)), the visibility of tracks by diffraction contrast in dark field is often poor. After sufficient etching to remove the amorphous layer but leave the tracks unetched, the track visibility is greatly improved. Using particle-bearing carbon films cemented to 200 mesh 'finder' grids, Barber et al (1970) have been able to follow the progress of etching of solar flare particle tracks in lunar fines returned by the Apollo 11 and 12 missions. More recently, we have thus established that, with appropriate etching conditions, all of the tracks visible by

diffraction contrast can be etched. Figure 2 shows a high density of finely etched tracks in a lunar pyroxene fragment.

(b) Since sputter-etching is best performed from two sides of a grain simultaneously and minerals have been found to have low sputtering yields, the choice of a mounting medium for large grains is limited. Epoxy cements and plastics are not suitable because they sputter faster than minerals. For some purposes, it is feasible to use sealing glasses into which grains can be introduced by flash heating to ~500 °C. But even if such heating can be tolerated, glass mounts are very brittle so that grinding, prior to ion-thinning, usually results in the loss of some samples. Moreover, the sputtering rates for glasses are not as low as those of the most resistant minerals, which include the pyroxenes.

A satisfactory mount has proved to be finely-ground aluminum oxide packed tightly into low viscosity epoxy resin. Aluminum oxide has a sputtering yield less than most minerals, as shown by Wehner et al (1963), and comparable to that of the clinopyroxenes for 6kV argon ions. Thus, provided that the powder is closely compacted and in intimate contact with the sample grains, the composite mount will hold together down to thicknesses ~1μm. The Spurr (1969) low viscosity diepoxide formulation has been used with 1μm polishing alumina in work on lunar fines at Berkeley. Figure 3 is a dark field micrograph of tracks (unetched) near to the original surface of a 630μm diameter particle in a sputter-etched composite mount.

ACKNOWLEDGMENTS

I would like to thank Profs. P.B. Price and G. Trilling for their hospitality during my year's leave at the University of California, Berkeley and to thank Prof. G. Thomas for giving me access to the 650 kV electron microscope.

REFERENCES

D.J. Barber (1970). J. Mat. Sci. 5, 1-8.

D.J. Barber, I. Hutcheon and P.B. Price (1971). Science, 171, 372-374.

J.C. Dran, L. Durrieu, C. Jouret and M. Maurette (1970). Earth Planet. Sci. Letters 9, 391-400.

J.D.C. McConnell (1970). Physical Methods in Determinative Mineralogy, (ed. Zussman), 335-370, Academic Press, New York.

A.R. Spurr (1969). J. Ultrastructure Research, 26, 31-43.

N.J. Tighe (1968). Proc. 15th Sagamore Army Materials Research Conference, Racquette Lake, New York.

A.K. Wehner, C. Kenknight and D.L. Rosenberg (1963). Planet Space Sci. 11, 885-895.

FIGURE CAPTIONS

Figure 1 Etched tracks of solar flare nuclei in a heavily etched (1 part HF : 2 parts H_2SO_4 : 280 parts H_2O - 1 minute) particle from the lunar soil encased in an evaporated carbon film. Note the carbon envelope showing the original shape of the particle and the earlier presence of two adhering smaller fragments of lunar dust.

Figure 2 Finely etched solar flare particle tracks (track density $6 \times 10^{10}/cm^2$) in a pyroxene fragment from the lunar soil.

Figure 3 Dark field micrograph of unetched solar flare particle tracks in a large (630μm diameter) pyroxene fragment from the lunar soil which was sputter-etched after incorporation into a composite mount.

(8)

PROC. 25th ANNIVERSARY MEETING OF EMAG, INST. PHYSICS, 1971

Solar Flare Particle Tracks in Lunar and Meteoritic Minerals

D.J. Barber* and P.B. Price†

*Physics Department, University of Essex, Colchester and †Physics Department, University of California, Berkeley, California, U.S.A.

We have investigated the occurrence of tracks of heavily-ionizing particles in lunar fines, rocks and meteorites, using mainly high voltage (650 kV) electron microscopy. The tracks are attributed to energetic nuclei, largely Fe, most of which have emanated from the sun during flares. The distributions of these tracks of ancient nuclei in lunar and meteoritic minerals allow us to made deductions about the formation and erosion of the lunar surface and the history of meteorites.

Lunar soil particles less than ~5μm dia. were examined both as received and after slight etching. Tracks are visible in diffraction contrast (fig. 1) but the strain fields are smaller than for dislocations; etched tracks are more readily visible (Barber et al. 1971), but minerals require a variety of etching conditions. Using both etching and dark field we now conclude that ~20% of small particles possess very high densities of tracks ($>10^8$ mm^{-2}). Significant numbers of track-rich grains occur at all depths in the Apollo 12 600 mm core sample. The irradiated grains are variable in shape and apparently include all the common lunar minerals. A frequent feature of track-rich grains, although not a guarantee of high track content, is the presence of an amorphous layer, some 500 Å thick, attributed to accumulated damage from solar wind ions. High track densities and the amorphous layer have also been reported by Borg et al. (1970) and Dran et al. (1970). Although X-ray studies of the smallest fines indicate only poor crystallinity, this must be largely attributed to the presence of glassy fragments and the amorphous layers. The interiors of most of the irradiated grains give single crystal electron diffraction patterns and structural defects (other than tracks and exsolution lamellae) are rare. We find that etching, even if insufficient to etch tracks, improves diffraction contrast by removing the amorphous layer. Some grains which contained no tracks exhibited black spots, reminiscent of displacement damage. A few of these grains were identified as troilite, FeS. The spottiness cannot be associated with irradiation for certain because fine-scale precipitation effects occur in some lunar minerals.

Coarse fines (0.1-1 mm dia.) were made into composite mounts and sputter-etched to suitable thicknesses for t.e.m. (Barber 1971). We have studied about 50 large grains but we have so far failed to locate such high track densities (> 10^9 mm^{-2}) as found commonly in the smallest fines. However, the track distribution is otherwise unremarkable; from our limited statistics the track gradient appears similar to that in lunar rock (see below). In a few grains we found many small bubbles or voids, which were not present on traversing a few microns in from the surfaces. These may be precipitated gas from solar wind ions, nucleated in some subsequent brief rise in temperature, perhaps during splashing with molten glass. Figure 2 shows bubbles (reversed in contrast on either side of thickness fringes) together with lamellar precicipitates (faint orthogonal lines) in ölvospinel.

Using a replica method on an etched vertical section through the surface of rock 12022, the variation of track density with depth has been measured to a depth of 3 mm, where optical microscopy could be used. A region was chosen where there was a large pigeonite crystal, since reliable track etching occurs with good definition in pyroxenes. Figure 3 shows part of the carbon replica. The track counts were normalized to optical data, since we have found electron microscopy is able to detect shallow etch pits (probably at dislocations, precipitates and spallation tracks) which are not seen optically. The track density at the surface of the rock was a little less than 10^8 mm^{-2}. The track gradient was then converted to an energy spectrum for Fe-ions and compared with the spectrum

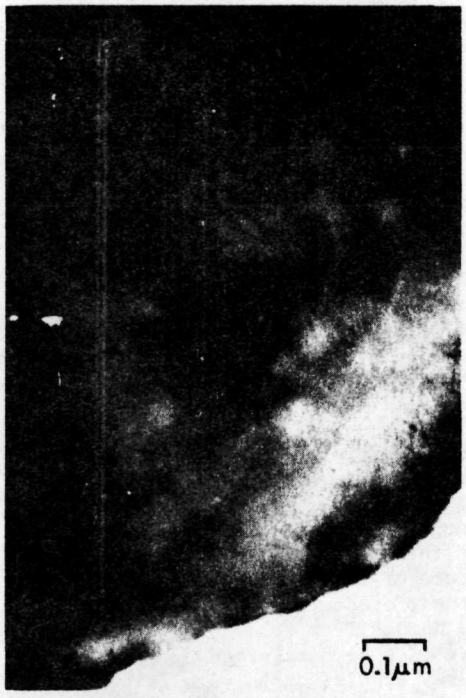

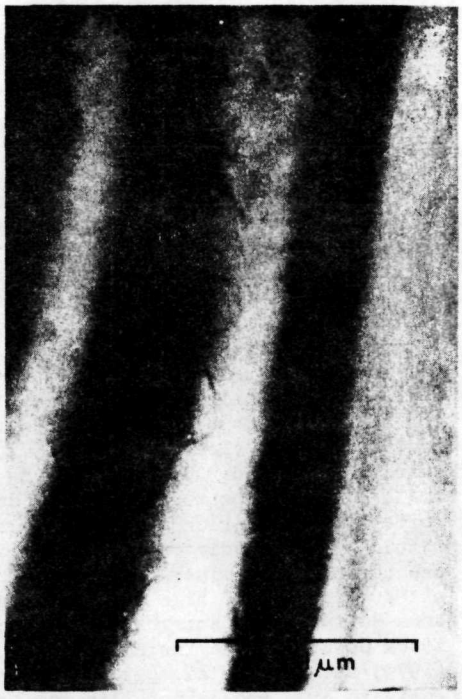

Figure 2

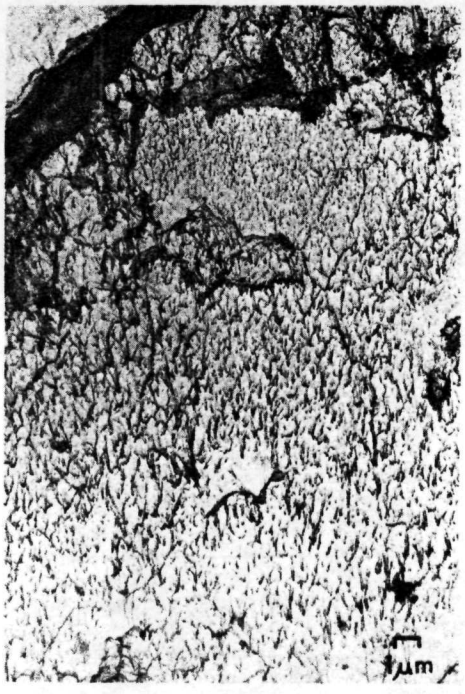

Figure 3

Figure 4

deduced from track data from the glass filter of the Surveyor 3 camera (exposed to solar flares for 2.6 years during the active part of the solar cycle). From the comparison it was deduced that the erosion rate of rock 12022 was ~3Å/year, suggesting that microcratering rather than sputtering is the predominant erosion process. The Surveyor filter results also partially explain the very high track densities in the fines. At first these high track densities were thought to be unique and were hard to accept without invoking either (i) the production of tracks by fluxes of suprathermal ions (Borg et al. 1970) or (ii) an extra-lunar component in the soil or a more active sun in the past (Barber et al. 1971). The filter results show that the difficulty is largely illusory because the actual flux of Fe ions is greater than that deduced from measured H and He fluxes and the known photospheric abundances (Price et al. 1971).

Track densities up to 10^7 mm^{-2} have been found by s.e.m. and optical microscopy in gas-rich meteorites (Pellas et al. 1969; Lal and Rajan, 1969). Our t.e.m. studies on sputter-thinned foils from the dark portions of gas-rich meteorites show that about 5-10% of the grains in at least some of these meteorites have track densities >10^8 mm^{-2}. We have found such densities in the Staroe Pesjanoe, Kapoeta and Fayetteville meteorites; fig. 4 shows tracks in the latter. In Fayetteville, many of the largest grains are olivine and rather more than 10% are track rich. Figures 5a and 5b are dark field micrographs of olivine with and without tracks, respectively. Fayetteville is particularly suited to track studies by t.e.m. because it is fine-grained and free from cracks and distortions caused by mechanical shock. Although there is often no sign of a layer between the grains, we have never observed tracks to pass from grain to grain. Tracks also occur in small isolated euhedral grains in a fine glass-like matrix. Small track-rich grains are hard to find in Kapoeta, which is heavily shocked and does have much glass between the grains. Most of the evidence from Fayetteville indicates that the grains were irradiated before the meteorite was assembled and that cohesion was produced at fairly low temperatures. However, in some regions of the meteorites one sees smooth grain boundaries (direct crystal contact) which are hard to explain without recourse to thermal equilibration.

We have also sought tracks in the gas-rich carbonaceous chondrites, Murray and Orgeuil. So far none have been found and other features indicate that the meteorites have been strongly heated at some time: there are 120° grain boundary junctions and few dislocations are present in the larger crystallites. Figure 6 shows part of Murray where the crystal contact is poor and there is a substantial amount of fine-grained 'altered' fabric. In contrast, Fig. 7 shows another part where the grain structure is more like that of a well-sintered ceramic. We have also examined the magnetite particles in Orgeuil which have been discussed by Kerridge (1970): Some of the polygonal grains are structureless, some are spherulitic and some have spotty contrast, as shown slightly in fig. 8. The dark field image shows that magnetite is also finely distributed in the altered matrix. Most of the fabric of Orgeuil is altered and porous.

Barber D J, Hutcheon I and Price P B 1971 Science 171 372
Barber D J 1971 Amer. Min. in press
Borg J, Dran J C, Durrieu L, Jourette C and Maurette M 1970 Earth Planet. Sci. Lett. 8 379
Dran J C, Durrieu L, Jourette C and Maurette M 1970 Earth Planet. Sci. Lett 9 391
Kerridge J F 1970 Earth Planet. Sci. Lett. 9 299
Lal D and Rajan R S 1969 Nature 223 269
Pellas P, Poupeau G, Lorin J C, Reeves H and Audouze J 1969 Nature 223 272
Price P B, Hutcheon I, Cowsik R and Barber D J 1971 Phys. Rev. Lett. in press

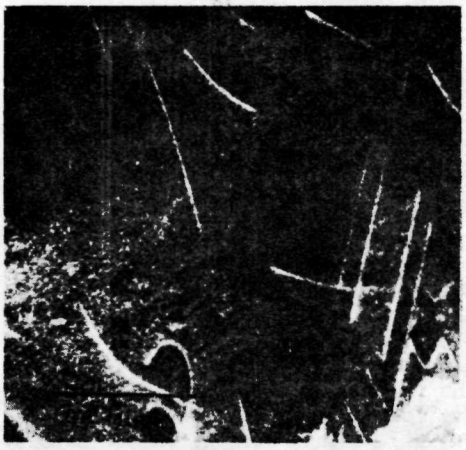

Figure 5(a)

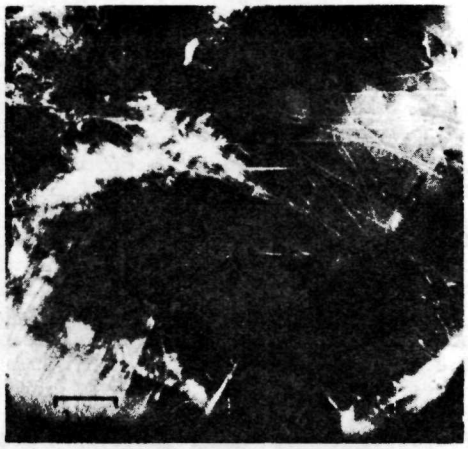

Figure 5(b)

Figure 6

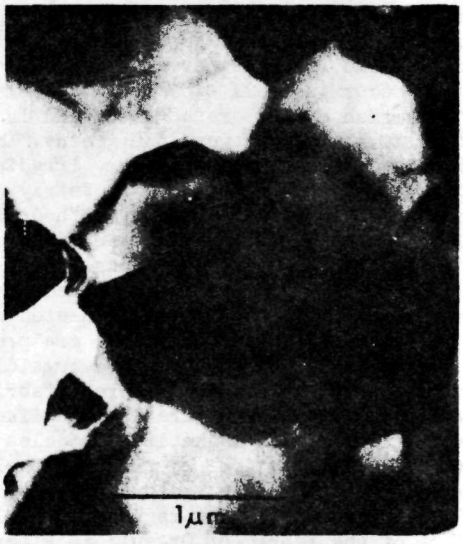

Figure 7

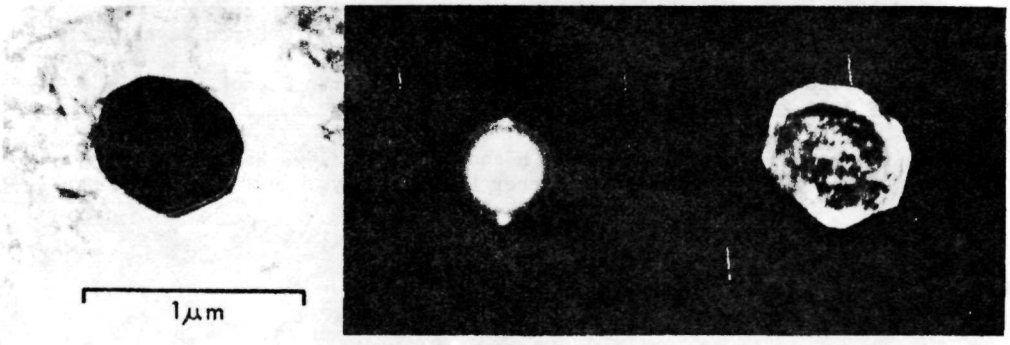

Figure 8